A modelling study of air quality impact of odd-even day traffic restriction scheme before, during and after the 2008 Beijing Olympic Games

H. Cai and S. D. Xie*

College of Environmental Science and Engineering, State Key Joint Laboratory of Environmental Simulation and Pollution Control, Peking University, Beijing, People's Republic of China

Abstract. Systematic air pollution control measures were designed and implemented to improve air quality for the 2008 Beijing Olympics. This study focuses on the evaluation of the air quality impacts of a short-term odd-even day traffic control scheme (TRS) implemented before, during and after the Games, based on modelling simulation by a well validated urban-scale air quality model. Concentration levels of CO, PM_{10}, NO_2 and O_3 were predicted for the pre- (10^{th}-19^{th}, July), during- (20^{th} July-20^{th} September) and post-TRS (21^{st}-30^{th}, September) periods, based on the on-line monitored traffic flows on a total of 334 road segments constituting the 2^{nd}, 3^{rd}, 4^{th} Ring Roads (RR) and the major Linkage Roads (LRs) that were subject to the TRS policy and distributed around the main urban area of Beijing, and on the hourly sequential meteorological data from a representative Observatory. Subsequently, we used the predictions and observations at a roadside air quality monitoring site to evaluate the model, based on a widely used statistical framework

* Corresponding author. Tel.: +86 10 62755852; fax: +8610 62751927.
E-mail address: sdxie@pku.edu.cn.

for model evaluation, as well as on the dependence of model performance on time-of-the-day and on wind direction, and the model predictions turned out satisfactory. Results showed that daily average concentrations on the 2nd, 3rd, 4th RR and LRs during the TRS period decreased significantly, by about 35.8%, 38.5%, 34.9% and 35.6% for CO, about 38.7%, 31.8%, 44.0% and 34.7% for PM_{10}, about 30.3%, 31.9%, 32.3% and 33.9% for NO_2, and about 36.7%, 33.0%, 33.4% and 34.7% for O_3, respectively, compared with the pre-TRS period. Besides, hourly average concentrations were also reduced significantly, particularly for the morning and evening peaks for CO and PM_{10}, for the evening peak for NO_2, and for the afternoon peak for O_3. Consequently, both the daily and hourly concentration level of CO, PM_{10}, NO_2 and O_3 conformed to the CNAAQS (China National Ambient Air Quality Standards) Grade II during the Games. Besides, a notable ozone weekend effect was revealed for the pre- and post-TRS periods, and was virtually removed for the during-TRS period. In addition, notable reduction of concentration levels were achieved in different regions of Beijing in response to the TRS policy, with the air quality in the downwind northern and western regions improved most significantly. The TRS policy was therefore effective in improving short-term air quality in Beijing during the Games.

1. Introduction

Beijing, the capital city of China and the host city of the 2008 Olympic Games, has a population of over 18 million and meanwhile suffers serious air pollution constituted

by high concentration levels of PM_{10}, CO, SO_2 and NO_2. Particularly, PM_{10}, with its high daily and annual concentrations on average, remained the primary air pollutant in Beijing since 2000 (Beijing EPB, 2009). The PM_{10} annual average concentration in Beijing has been staying at a high level, fluctuating around 160 $\mu g/m^3$ during the period of 2001-2006, and began to decrease in the following two years as a result of various control measures, with the annual average concentration in 2008 still exceeding 120 $\mu g/m^3$ (Beijing EPB, 2009), which was about 20% higher than the China National Ambient Air Quality Standards (CNAAQS) Grade II (100 $\mu g/m^3$) and six times the latest World Health Organization (WHO) Air Quality Guidelines (WHO, 2005). Of the major anthropogenic sources of atmospheric particulate matters in the mega cities (e.g. Beijing, Shanghai, Guangzhou) in China, on-road vehicular emissions is an important and perhaps the fastest growing one (Chan and Yao, 2008). Although the source contributions of motor vehicles to PM_{10} and $PM_{2.5}$ in Beijing revealed by the PMF (positive matrix factorization) methodology were only 5% (Xie et al., 2008) and 6% (Song et al., 2006b), respectively, motor vehicles were a major contributor to ambient concentrations of nitrogen dioxide (NO_2)/nitrogen oxides (NO_x) and carbon monoxide (CO), according to a conclusion that on-road vehicle source had contributed 76.5% and 68.4% of the CO and NO_x concentrations, respectively, in urban atmosphere of Beijing in 1995 (Hao et al., 2001). Moreover, traffic congestion and traffic-related air pollution has been a serious issue in urban Beijing with the vehicle population increasing dramatically at a daily rate of over one

64 thousand, reaching over 3.5 million by the end of 2008. The booming economic
65 prosperity and substantial increase of vehicle population has resulted in the
66 exponential growth of vehicular emissions of CO, PM_{10}, NO_x, VOC (volatile organic
67 compounds) (Cai and Xie, 2007), as well as speciated VOC emissions containing
68 highly reactive and toxic pollutants in the atmosphere of Beijing (Cai and Xie, 2009).
69 In order to improve effectively the air quality and traffic condition in Beijing, a
70 Sino-Italian environmental protection program based on Intelligent Traffic System
71 and Traffic Air Pollution (ITS-TAP) monitoring was launched between the Italian
72 Ministry for the Environment and Territory and Beijing Municipal Government in
73 2005. Moreover, the Beijing Municipal Government had committed to the
74 international society that air quality in Beijing would be improved and be better than
75 before, satisfying the CNAAQS and WHO Air Quality Guidelines during the 2008
76 Olympic Games. To fulfill the air quality commitment during the Games, the
77 government implemented a list of control measures, including greening of bare land
78 by afforestation both in Beijing and some surrounding provinces, enhancing the
79 utilization of natural gas to replace coal for heat supply and residential cooking,
80 closing or relocating heavy industrial polluters (e.g., the Capital Steel Company),
81 reducing local power generation by importing electricity from the surrounding areas,
82 promoting abatement and removal technologies for sulfur dioxide and particulate
83 matter from industrial point sources, suspending construction activities as well as
84 imposing strict control of VOC evaporation at gas stations (Wang et al., 2009a). In

addition, air pollution sources were strictly controlled in the surrounding provinces of Tianjin, Hebei, Shanxi, Neimenggu and Shandong to prevent regional contribution through long-range transportation, based on the evidences obtained in previous studies (Streets et al., 2007 and Wang et al., 2008a). Also, five control schemes for controlling vehicular emissions were implemented: issuance of new automobile emissions standards; decommissioning of high emissions vehicles, buses and taxis; recovery of fuel vapors at pumping stations and from tankers; banning of non-local heavy duty diesel trucks within the Beijing Administrative area; and control of emissions from small stationary diesel generators (COC, 2008). Meanwhile, Beijing took the lead in China to adopt the Euro-IV emission standard to reduce vehicle emissions of air pollutants five months before the Olympic Games. Particularly, an odd-even day traffic restriction scheme (TRS), a control measure that was demonstrated to be effective in Atlanta (Fang et al., 2009), was enforced for two months from 20th July to 20th September, 2008, to help ease congestion and improve air quality during the Olympics and Paralympics. Consequently, the UAB had a distinct characteristic of source emissions compared to usual periods, as emissions from sectors other than on-road vehicles were expected to decrease significantly, with on-road vehicles becoming the major source for air pollution in that particular period, due to their huge population even after the TRS policy was in effect. Previously, Cheng et al. (2008) demonstrated that the four-day traffic restrictions in Beijing during the Sino-African Summit in early November 2006 resulted in significant

106 temporary reductions in concentrations of NO_x and particulates in the city. Besides,
107 Westerdahl et al. (2009) conducted in-situ measurements and concluded that a
108 four-day traffic control experiment from 17^{th}-20^{th} August, 2007 conducted by the
109 Beijing Government as a pilot to test the effectiveness of the proposed odd-even day
110 TRS was effective in reducing extreme concentrations that occurred at both on-road
111 and ambient environments. Wang et al. (2009a) evaluated the air quality impacts of
112 the 2008 Beijing Olympic Games, focusing on the measurement of on-road black
113 carbon emission factors and the evaluation of reduction of black carbon
114 concentrations. Wang et al. (2009b) conducted a modelling analysis, aiming to
115 assess the effectiveness of various emission restrictions implemented during the 2008
116 Beijing Olympics on the ozone air quality at a rural site of Beijing during the period.
117 As the control measures for sectors other than on-road vehicles were constantly in
118 effect and remained the same for the pre-, during- and post-TRS periods, this study
119 intends to seize this unique opportunity to study the air quality impact and
120 effectiveness of the TRS policy, by adopting an integrated urban-scale modelling
121 system with online-monitored data of on-road traffic flows at a high temporal
122 resolution of two seconds from the ITS-TAP system, and based on the analysis of the
123 short-term air quality variation near the simulated roads in response to the TRS policy.
124 Model-based simulation has been one of the major tools for air quality assessment,
125 air pollution diagnosis and evaluation of pollution control policies at the urban,
126 regional and global levels. A few dispersion models have been widely applied to

127 simulate urban air pollution from traffic-related emissions, e.g. OSPM (Berkowicz,
128 2000; Kukkonen et al., 2001; Assael et al., 2008; Berkowicz et al., 2008), CALINE
129 (Levitin et al., 2005; Yura et al., 2007), CALPUFF (Wang et al., 2006), ISCST3 (Elbir,
130 2002; Ying et al., 2007; Sharma and Chandra, 2008). ADMS-Urban, a well tested
131 and intensively validated quasi-Gaussian dispersion air quality model, which is
132 widely used for regulatory purposes in the UK and used in the investigation and
133 assessment of air pollution mitigation and control strategies in many cities of China
134 (Carruthers et al., 1994; Bennett and Hunter, 1997; McHugh et al., 1997; Carruthers et
135 al., 1999; Carruthers et al., 2000a; Carruthers et al., 2001; Riddle et al., 2004;
136 McHugh et al., 2005; Hirtl and Baumann-Stanzer, 2007), has recently been validated
137 by the Ministry of Environmental Protection of China as one of the three
138 recommended dispersion models (the others are the US EPA's CALPUFF and
139 AERMOD) for air quality impact assessment (MEPC, 2009), and by a commercial
140 system of street-level air quality forecasting which was launched in Beijing in July,
141 2008 (BeijingAir, 2008). Moreover, ADMS-Urban has some features especially
142 tuned to obtain best performance on urban areas (CERC, 2003), which is mostly due
143 to its advantages over other recommended models, like the up to date
144 parameterization of atmospheric boundary layer structure based on the
145 Monin-Obukhov length and the boundary layer height, and the Gaussian
146 concentration distributions in stable and neutral conditions, but non-Gaussian vertical
147 distributions in convective conditions to take into account the skewed structure of the

148 vertical component of the turbulence. Furthermore, it is particularly convenient to
149 set up on-road emissions, and to define the road source geometry and the output
150 presentation in an accurate way, by means of the nested GIS tool (Arcview or
151 Mapinfo). Thus, ADMS-Urban was adopted in this study to simulate and assess the
152 air quality impact in UAB in response to the TRS policy before, during and after the
153 2008 Beijing Olympic Games. Firstly, the modelled results were evaluated with the
154 measurement data from a typical roadside air quality monitoring site. Subsequently,
155 the ambient concentrations of CO, PM_{10}, NO_2 and O_3 at a height of 1.5 metres were
156 calculated for the periods of pre-TRS (10^{th}–19^{th} July, 2008), during-TRS (20^{th} July-
157 20^{th} September, 2008) and post-TRS (21^{st}-30^{th} September, 2008), respectively, based
158 on traffic flows on the dense network of 2^{nd}, 3^{rd} and 4^{th} Ring Roads (RR) and Linkage
159 Roads (LRs, including major intercity expressways and intercity roads between RRs),
160 followed by an assessment of the temporal and spatial variation of air quality impacts
161 in response to the TRS policy.

162 **2. Methods and data**

163 2.1 Description of study domain, urban and background monitoring sites, and
164 receptors

165 The study domain, the main UAB, covers the 2^{nd}, 3^{rd} and 4^{th} RR, which were 32.7,
166 48.0 and 65.3 kilometers long, and had six, six to eight and eight lanes, respectively,
167 as well as the major LRs mainly having eight lanes. These simulated roads were the
168 main roads of UAB with the majority of traffic flows in it. About 62% of Beijing is

mountainous area located in the west, the north and the northeast. Thus, the local wind field has a clear diurnal variation, with northeasterly and southeasterly winds dominating in the daytime and southeasterly wind dominating in the night. The Chegongzhuang (CGZ) air quality monitoring site, which was located five kilometers west of the West 2nd RR and was on a corner (geographical coordinates: 39°55'53"/N, 116°19'38"/E) of a crossroad where a five-lane North-South oriented street and a six-lane West-East oriented street intersected with high traffic flows, had a sampling height of about 4.5 metres from ground and had been well maintained with routine calibration of the measurement equipment by the Beijing Municipal Environmental Monitoring Centre during the Games as a traffic monitoring site. This site provided the model evaluation data of hourly concentrations of CO, $PM_{10,}$ NO_2 and O_3 for 10^{th}-20^{th} July and 10^{th}-20^{th} August, 2008. To assure the accuracy of the model predictions, it is important to account for significant underlying, or 'background' levels of pollutants in the atmosphere, and to account for any sources of pollution that are not otherwise included in the model run. Therefore, we selected the background diurnal profiles of CO, PM_{10} and NO_2 for the whole evaluation period from Dingling (DL) air quality monitoring station, which was approximately 42 kilometers north from the CGZ air quality monitoring site and was in the suburban area with very few motor vehicles. Background measurements from DL could reflect well the real situation of the air quality in the UAB during the Games, which was expected to be influenced mainly by local on-road vehicles, with a minor contribution from other

well controlled sources like power plants and polluting industrial plants, construction sites and gas stations both in Beijing and the surrounding provinces during the Games (Wang et al., 2009a). Therefore, it is reasonable to make comparisons between modelled predictions and measurement data at CGZ for the model evaluation. For O_3, a major secondary air pollutant, we used the measurement data from Shangdianzi (SDZ) regional atmospheric background monitoring site, one of the four regional atmospheric background monitoring sites in China and located about 150 kilometres northeast of Beijing (40°39'/N, 117°07'/E). Measurement data from the SDZ background measurement site are free of influence by motor vehicles and represent the background characteristic of atmospheric constitutes in northern regions of China including Beijing (Liu et al., 2007). Therefore, this site is suitable for providing the background O_3 measurement data for this modelling study. Due to the lack of the measurement data from this site for the summer in 2008, we have adopted the measurement data in SDZ for the summer periods in 2004 (Liu et al., 2006) and in 2006 (Liu et al., 2008) as a substitute, considering the generally accepted understanding of the relatively constant feature of background concentrations within a short time peirod. Finally, we used the averaged daily profiles for July, August and September based on the 2004 and 2006 data from SDZ as the background O_3. To reflect the variation of air quality in the areas near the dense network of simulated roads, 31 representative receptors located along the 2^{nd}, 3^{rd} and 4^{th} RR and the LRs were chosen, where the hourly concentrations of CO, PM_{10}, NO_2 and O_3 were

211 simulated for the pre-TRS, during-TRS and post-TRS periods. Besides, receptors
212 located in different regions of the UAB were used to capture the air quality variation
213 in different parts of the UAB in response to the TRS policy. The road network of
214 Beijing and the road sources of RR and LRs distributed in the study domain,
215 including the locations of the CGZ, DL and SDZ air quality monitoring sites and the
216 representative receptors, are shown in Figure 1.

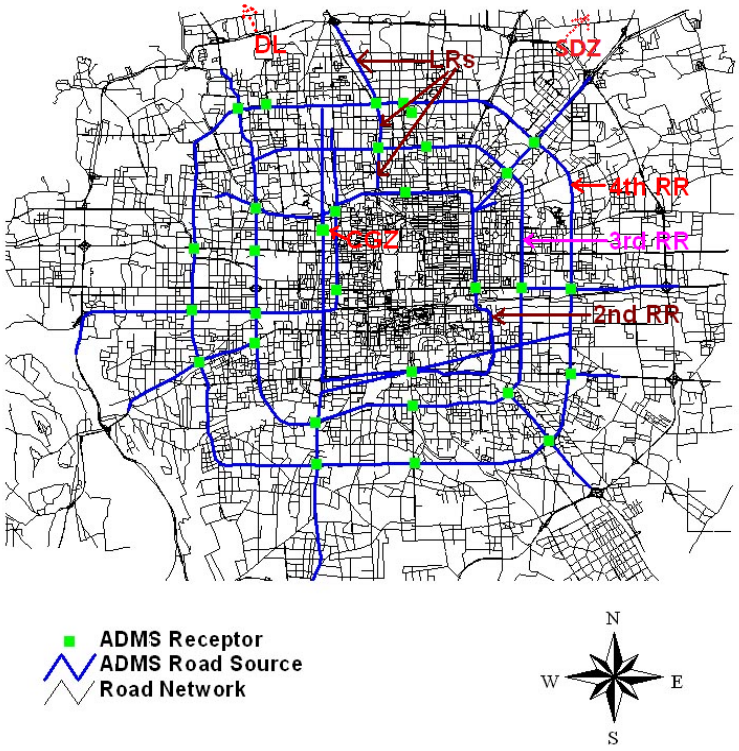

217

218 Fig. 1. Map of the road network of UAB, road sources of RR and LRs, CGZ, DL and
219 SDZ air quality monitoring sites, and representative receptors distributed in the study
220 domain.

221 2.2 ADMS-Urban model set up

222 The ADMS-Urban model, developed by Cambridge Environmental Research
223 Consultants (CERC, 2009), is a quasi-Gaussian dispersion model for the dispersion

simulation of pollutants released from industrial, domestic and road traffic sources in urban areas. Particularly, ADMS-Urban has an advantage over other urban-scale dispersion models as it characterizes the boundary layer structure based on the Monin-Obukhov length and boundary layer height rather than the more imprecise characterization achieved with the Pasquill-Gifford stability parameter (CERC, 1999).

Various parameters which need to be set for running ADMS-Urban include surface roughness, the latitude of the modelling area, minimum Monin-Obukhov length, the chemical reaction scheme, the meteorological data and the height of recorded wind, the background data, the source data including the road width, elevation, and the canyon heights in case of modeling street canyons, the time varing factors for weekdays, Saturdays and Sundays, the road geometry indicated by the geographical coordinates of the constituting nodes, and the output parameters like the pollutants included, the number of grids for the modelling area and the heights of concentrations to be calculated for the modelling domain and the receptors, respectively.

2.2.1 Descriptive parameters, chemical reaction scheme and deposition

Descriptive parameters were used to describe the modelled area, for example, the surface roughness characterised the surrounding area in terms of the effects it would have on wind speed and turbulence, which is one of the key components of the modelling. The values chosen for some representative parameters for the modelling domain is given in Table 1.

Table 1.

Parameters	Value

Surface roughness (m)	1.0
Latitude of the modelling area (°)	40
Minimum Monin-Obukhov length (m)	30
Pollutants included	NO_x, NO_2, CO, PM_{10} and O_3
Number of grids	10000
Horizontal resolution	$0.35km \times 0.35km$
Height of concentrations to be calculated (m)	1.5

The value of surface roughness was chosen based on some local studies (Hu, 1994; Zhang and Chen, 1997; Lu et al., 2002) and on the recommended value for modelling big cities, which is 1.0 metre. The value of 30 metres was chosen as the minimum Monin-Obukhov length as recommended by ADMS-Urban for cities.

ADMS-Urban has two chemistry options to calculate NO_2 and O_3 concentrations. The first option uses the empirical function (Derwent and Middleton, 1996). The second one is based on a chemistry scheme known as the Generic Reaction Set (GRS) (Venkatram et al., 1994), which is a semi-empirical model that simplifies photochemical reactions using a set of parameters derived from observations. The GRS scheme can work when background NO_x, NO_2 and O_3 data, as well as hourly sequential meteorological data including cloud cover are available. In ADMS-Urban, the primary NO_2/NO_x emissions fraction is assumed constant (5%) with the GRS scheme, and the NO_2 photo-dissociation coefficient is calculated using cloud cover data, in place of the radiation data. In this study, we adopted the GRS scheme to simulate the important reactions involving NO_x, VOC and O_3, since it has been demonstrated that the GRS scheme produced better results than the other option (D-M) (Vardoulakis et al., 2007).

The dry deposition process was considered by the dry deposition module of

263 ADMS-Urban, which is actually a resistance model dependent of the pollutant species,
264 the nature of the surface and the wind speed (CERC, 2009), while the wet deposition
265 process was ignored during the modelling since the dry air and lack of rain during the
266 evaluation period were not favorable for wet deposition of pollutants (Wang et al.,
267 2008c).
268 2.2.2 Emissions, road geometry, traffic flows, fleet compositions and emission factors
269 By implementation of high intensity of administrative regulations for emission control,
270 the natural, industrial, agricultural, construction, biomass burning and residential
271 emissions were expected to be reduced significantly and become sparse, and the
272 compilation of a complete emission inventory including the scarce and scattered
273 emissions from sectors other than on-road vehicles was very difficult, and the
274 inaccuracy of modelling could be considerable if all sources were considered.
275 Furthermore, emissions from other minor roads were not considered either, partly
276 because traffic flows on these roads were relatively less than those on the monitored
277 main roads, and partly because emissions from the minor roads were difficult to
278 quantify accurately due to the lack of an online continuous monitoring system for
279 traffic flows. Most importantly, variations in air quality near the simulated roads,
280 which were reflected by the receptors located near the monitored main roads
281 distributed around the UAB, were focused on and analyzed, to fulfill the objective of
282 evaluating the air quality impact and effectiveness of the TRS policy, rather than
283 analyze the air quality variations throughout the UAB, which benefited from all

284 control measures including the TRS policy. Therefore, emissions considered in this
285 study only involved with the vehicular emissions from the dense network of
286 monitored main roads, with additional background information representing
287 contributions from other sources of pollution that were not included in the model run.
288 We believe this approach is a good substitute for a complete emission inventory that
289 was difficult to compile accurately and could probably raise large uncertainty, and is
290 reasonable to assure the credibility of modelling results and conclusions, particularly
291 when the primary objective of this study is concerned, although we admit that the
292 major drawback of not using a complete emission inventory in the simulations might
293 cause some inaccuracy in the absolute values of the predictions, particularly in the
294 areas near other ignored minor roads or away from the monitored major roads.

295 The 2^{nd}, 3^{rd} and 4^{th} RR, as well as the major LRs were separated into a total of 334
296 road segments, the lengths of which were automatically identified by Arcview, a
297 nested GIS (Geographical Information System) software of ADMS-Urban, by
298 recognizing the geographical coordinates of the road nodes constituting each segment.
299 The width of each road segment was manually input based on field surveys. Unlike
300 another study that focused on the traffic-related air pollution within twelve typical
301 street canyons of Beijing using the OSPM model (Wang and Xie, 2009), this study
302 focuses on the modelling of traffic-related air pollution around the UAB, and thus the
303 street canyon effect was not modelled, with further consideration on the fact that the
304 majority of roads in the UAB were not typical street canyons, of which the building

heights on both sides were expected to be at least three times of the road width.

Traffic flows on each of the road segments of the 2nd, 3rd and 4th RR were intensively monitored automatically every two seconds from 10th July, 2008 to 30th September, 2008 by the ITS-TAP system. The high temporal resolution traffic flow data were further processed to summarize the hourly traffic flow and the hourly average running speed on each of the monitored road segments for the whole assessment period.

For the quality assurance and control of the traffic data, we first screened out the abnormal maximum values of monitored driving speed, which were recorded as 240 km/h. We regarded this to be impossible and abnormal, with the confirmation by technical experts of the ITS-TAP system. Further, these abnormal maximum speeds were replaced by the average of the normal speeds on the adjacent road segments. Moreover, the major problem of the monitored traffic flow data was the missing data on certain road segments for some periods of time. Accordingly, we treated those hourly sequential data sets with a fraction of missing data over 10% by replacing them with the average of the traffic flows on the nearest upstream and downstream road segments, which had less than 10% of missing data. In addition, we eliminated the few days (6th, 13th, 14th, 24th and 28th, September) when large quantities of missing data were found (data missing by about 43%, 36%, 47%, 84% and 73%, respectively, for those days), due to the malfunction of monitoring cameras of the ITS-TAP system on many road segments during the days. In this way, we assured that the monitored

326 driving speed was proper, and traffic flows were relatively complete, with a possible
327 underestimation of less than 10%.

328 The on-line monitored traffic flow data consisted of two vehicle categories: long
329 vehicles which were constituted of buses and heavy duty vehicles, and short vehicles,
330 which were constituted of passenger cars and light duty vehicles. The further
331 split-up of the fleet on each of the road segments into these four categories were based
332 on the surveyed fleet composition of the manual traffic counts conducted by technical
333 assistants at the roadsides of 290 road segments in urban Beijing in 2004.

334 Three different sets of time-varying factors for diurnal traffic flows were identified
335 separately for weekdays, Saturdays and Sundays, based on average traffic counts of
336 all the road segments for each hour of the day throughout the assessment period.
337 These profiles were used to derive time-varying emission rates (g/km/s) on all road
338 segments for weekdays, Saturdays and Sundays, respectively, which are thought to
339 reflect variations in diurnal emissions due to road traffic congestion or improvement
340 in traffic conditions.

341 Continuous emissions of CO, PM_{10}, NO_x and VOC from vehicles on the monitored
342 roads were provided every hour for the model run. According to the definition of
343 emission rates, as expressed by Equation (1), the emissions, lengths of road segments
344 and travelling time of vehicles are needed, to calculate the emission rates of CO, PM_{10},
345 NO_x and VOC on each road segment. More specifically, emission rates can be
346 calculated based on four parameters: emission factors (*EF*), vehicle population (*VP*),

lengths of road segments (L) and driving speed of vehicles (v), as shown by Equation (4), based on Equations (2-3). Traffic flows derived from the ITS-TAP system included the vehicle population of various vehicle types and the corresponding driving speeds on each segment. Emission factors of each pollutant from various vehicle categories were calculated by COPERT, a European emission factor model (EEA, 2000), based on the average running speed, ambient temperature and fuel property for a given vehicle category. The travelling time (t) on each road segment was calculated based on the speeds and road lengths that were automatically identified by Arcview, a nested GIS (Geographical Information System) software of ADMS-Urban.

$$ER_s = \frac{E_s}{L_s \times t_s} \quad (1)$$

$$E_s = \sum_i EF_i \times VP_i \times L_s \quad (2)$$

$$t_s = \frac{L_s}{v_s} \times 3600 \quad (3)$$

$$ER_s = \frac{\sum_i EF_i \times VP_i \times v_s}{3600 \times L_s} \quad (4)$$

Where: ER_s is the emission rate on road segment s, expressed in *g/km/s*; E_s is the emission on road segment s; L_s is the length of road segment s; t_s is the time used to travel on the road segment s; EF_i is the emission factor of vehicle type i; VP_i is the vehicle population of vehicle type i; and v_s is the running speed of vehicles on road segment s.

Using the established methodology (Cai and Xie, 2007), emission factors of

367 passenger cars, light duty vehicles, heavy duty vehicles and buses at a typical urban
368 running speed of 20 km/h in Beijing were calculated, as shown by Table 2.
369 Particularly, emission factors of each vehicle category on each road segment were
370 updated in accordance with the temporal variation of running speed to improve the
371 accuracy of source emission estimation.

372 Table 2. Emission factors (g/km) for passenger cars, light duty vehicles, heavy duty
373 vehicles and buses at a typical urban running speed of 20 km/h in Beijing, calculated
374 by COPERT and from literature reports.

	PM_{10}	CO	NO_x	VOC
Passenger cars	0.015a	5.99	0.44	0.35
Light duty vehicles	0.015a	11.28	0.82	0.47
Heavy duty vehicles	2.94a	2.22	2.72	0.91
Buses	2.94a	4.76	10.54	0.87

375 a: from Wang et al. (2001), as COPERT assumes gasoline vehicles do not emit
376 particles.

377 As for ozone, a secondary air pollutant, its model-predicted concentrations over the
378 simulated domain were based on the background measurement from SDZ background
379 monitoring site and the results of the GRS chemical mechanism operated by
380 ADMS-Urban, given the information of precursor pollutant emissions of NO_x and
381 VOC.

382 2.2.3 Meteorological data

383 Transport and dispersion of air pollutants in the atmosphere are influenced by regional
384 weather patterns. Operating on one hour intervals, meteorological data for

ADMS-Urban input files include wind speed, wind direction (including anemometer height), cloud cover, precipitation and temperature, which were used by the meteorological processor of ADMS-Urban to calculate the parameters for use in the model such as boundary layer depth and Monin-Obukhov length. The complete hourly meteorological data during the assessment period were obtained from the Beijing Capital International Airport Meteorology Observatory (ZBAA), which is about 20 km northeast from the Northeast 4th Ring Road and is known to be representative of the wind fields for UAB (Wang et al., 2009a). The daytime (8 am and 2 pm) and nighttime (8 pm and 2 am) wind roses during the period of 10th July – 30th September, 2008 are shown by Figure 2, which reveals that northeasterly and southeasterly winds dominated in the daytime while southeasterly wind dominated in the nighttime. Consequently, the UAB was dominated by the southeasterly and northeasterly winds in the whole day during the assessment period. Besides, the majority of wind speeds during the assessment period was less than 5.0 m/s, which indicate that the dissipation of air pollutants tended to be prolonged. It was also noted that the percentage of calm wind conditions was very low (0.5%) during the assessment period, which is in favor of ADMS-Urban's performance, since modelling of traffic sources in low wind speed conditions can lead to over-predictions and is sensitive to the minimum value of wind speed used (Carruthers et al., 2000b).

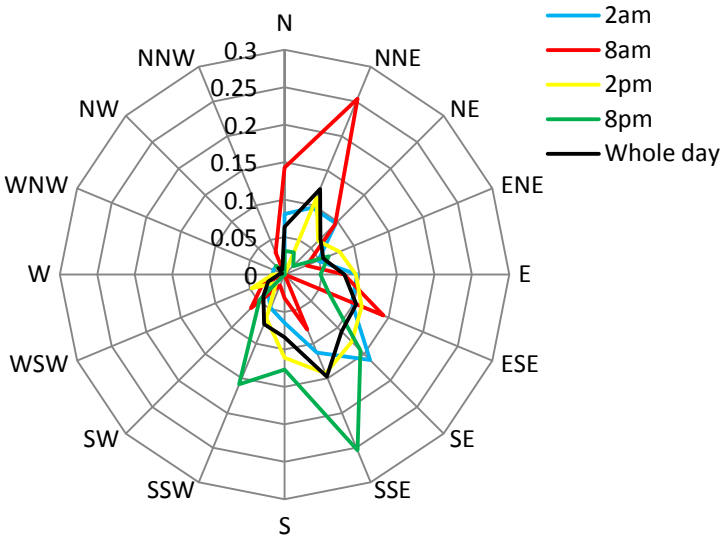

404

405 Fig. 2. Wind roses of wind directions at 2 am, 8 am, 2 pm, 8 pm and the whole day
406 from July to September, 2008. The radius indicates the frequency of wind observed
407 in each direction.

408 2.3 Model evaluation

409 The evaluation of the model performance was carried out by comparing the observed
410 hourly concentrations of CO, PM_{10}, NO_2 and O_3 at CGZ monitoring site with model
411 predictions for the periods of July 10^{th}-20^{th} and August 10^{th}-20^{th}, using the statistics
412 recommended by Hanna et al (1991, 1993), which have been adopted as a common
413 model evaluation framework for the European Initiative on ‘‘Harmonization within
414 Atmospheric Dispersion Modelling for Regulatory Purposes’’ (Olesen, 2001). The
415 statistical performance measures include (a) the fractional bias (FB) showing the
416 tendency of the model to overpredict or underpredict; (b) the normalized mean square
417 error (NMSE) showing the overall accuracy of the model; (c) the geometric mean bias
418 (MG) showing the mean relative bias and indicating systematic errors; (d) the

geometric variance (VG) showing the mean relative scatter and reflecting both systematic and random errors; (e) the Pearson correlation coefficient (R) describing the degree of association between observed concentrations and model results; and (f) the fraction of predictions within a factor of two of observations (FAC2). These statistical measures are defined as follows:

$$\mathrm{FB} = \frac{\overline{C_o} - \overline{C_p}}{0.5(\overline{C_o} + \overline{C_p})} \quad (5)$$

$$\mathrm{NMSE} = \frac{\overline{(C_o - C_p)^2}}{\overline{C_o}\,\overline{C_p}} \quad (6)$$

$$\mathrm{MG} = \exp(\overline{\ln C_o} - \overline{\ln C_p}) \quad (7)$$

$$\mathrm{VG} = \exp\overline{[(\ln C_o - \ln C_p)^2]} \quad (8)$$

$$R = \frac{\overline{(C_o - \overline{C_o})(C_p - \overline{C_p})}}{\sigma_{C_p}\sigma_{C_o}} \quad (9)$$

FAC2=fraction of data that satisfy $0.5 \leq \frac{C_p}{C_o} \leq 2.0$ (10)

Where: C_p are model predictions; C_o are observations; overbar($\bar{C}$) is the average over the dataset; and σ_C is the standard deviation over the dataset.

Since NMSE accounts for both systematic and random errors, it is helpful to partition NMSE into the component due to systematic errors, NMSEs, and the unsystematic component due to random errors, NMSEu. NMSEs, the minimum NMSE without any unsystematic errors, was defined by Hanna et al (1991) for a given value of FB as:

$$\mathrm{NMSEs} = \frac{4\mathrm{FB}^2}{4 - \mathrm{FB}^2} \quad (11)$$

The above statistical measures, however, do not provide information about the model performance under diurnal variation of weather and traffic conditions. For

that reason, the following qualitative performance measures have also been used: (i) diurnal pollution profiles to identify specific periods of the day when the model had good/poor performance; and (ii) pollution roses to compare predictions and observations at each of the wind directions and thus to show the model performance for different wind directions.

3. Results and discussion

3.1 Model evaluation

3.1.1 Overall model performance

The statistical evaluation results for CO, PM_{10}, NO_2 and O_3 based on the hourly predictions and observations are summarized in Table 3. The model predicted the concentrations of all pollutants reasonably well, with the FAC2 between 0.50 and 0.71. Besides, the FB statistic revealed that ADMS-Urban had a moderate tendency to underestimate NO_2 (FB=0.12) and O_3 (FB=0.31) concentrations, and had a moderate tendency to overestimate CO (FB=-0.22) concentrations and a slight overestimation of PM_{10} (FB=-0.0084) concentrations. The model showed satisfactory performance for NO_2 with a NMSE of 0.33, and moderate NMSE for CO, PM_{10} and O_3. Furthermore, the model performances indicated by NMSEs are very satisfactory for all pollutants, which agreed well with MG, the systematic error indicator. Besides, the model had a good performance for CO, PM_{10}, NO_2 and O_3 concentrations when considering both systematic and random errors as indicated by VG. Although the Pearson correlation coefficient for CO is relatively low (0.34), the R values for PM_{10},

461 NO_2 and O_3 were much higher. The R, however, is not a very robust measure due to
462 its sensitivity to a few outlier data pairs, and thus Willmott (1982) discourages the use
463 of R, because it does not consistently relate to the accuracy of predictions. Instead,
464 the FAC2, which is not overly influenced by either low or high outliers, is the most
465 robust performance measure.

466 Table 3. Statistical evaluation of model performance based on hourly predictions and
467 observations at CGZ monitoring site for the period of July 10^{th}-20^{th} and August
468 10^{th}-20^{th}, 2008.

	CO	PM_{10}	NO_2	O_3
Observed mean ($\mu g/m^3$)	1214.2	84.1	52.3	52.7
Predicted mean ($\mu g/m^3$)	1459.6	84.8	46.5	38.3
FB (ideal value: 0)	-0.22	-0.01	0.12	0.31
FAC2 (ideal value: 100%)	0.71	0.65	0.69	0.50
NMSE (ideal value: 0)	0.76	0.54	0.33	0.71
NMSEs (ideal value: 0)	0.05	0.00	0.01	0.10
MG (ideal value: 1)	0.92	0.81	1.07	3.33
VG (ideal value: 1)	1.57	2.27	1.42	4.51
R (ideal value: 1)	0.34	0.45	0.56	0.68

469 A scatter plot between the observed and predicted concentrations at CGZ is
470 presented in Figure 3, which illustrates the robust FAC2 statistic for CO, PM_{10}, NO_2
471 and O_3, respectively. There was a moderate overestimation for CO probably due to
472 the adoption of higher model-calculated emission factors, as shown by Figure 3 (a),
473 although the FAC2 for CO is high (0.71). As shown by Figure 3 (b), predicted and
474 observed PM_{10} concentrations agreed very well with each other, with its scatter plot
475 almost symmetrical. Figure 3 (c) reveals that a majority (69%) of predicted
476 concentrations fall within a factor of two of the observations for NO_2, with a slight

underestimation. The higher NO_2 observations might derive from the enhanced photochemical reactions of NO with oxidants such as peroxy radicals that were present either in the atmosphere or in vehicle exhaust (Kenty et al., 2007). Ozone was moderately underestimated, as revealed by Figure 3 (d), but was still satisfactorily predicted when taking into account the limitation of the simplified GRS scheme adopted in predicting secondary pollutant like ozone.

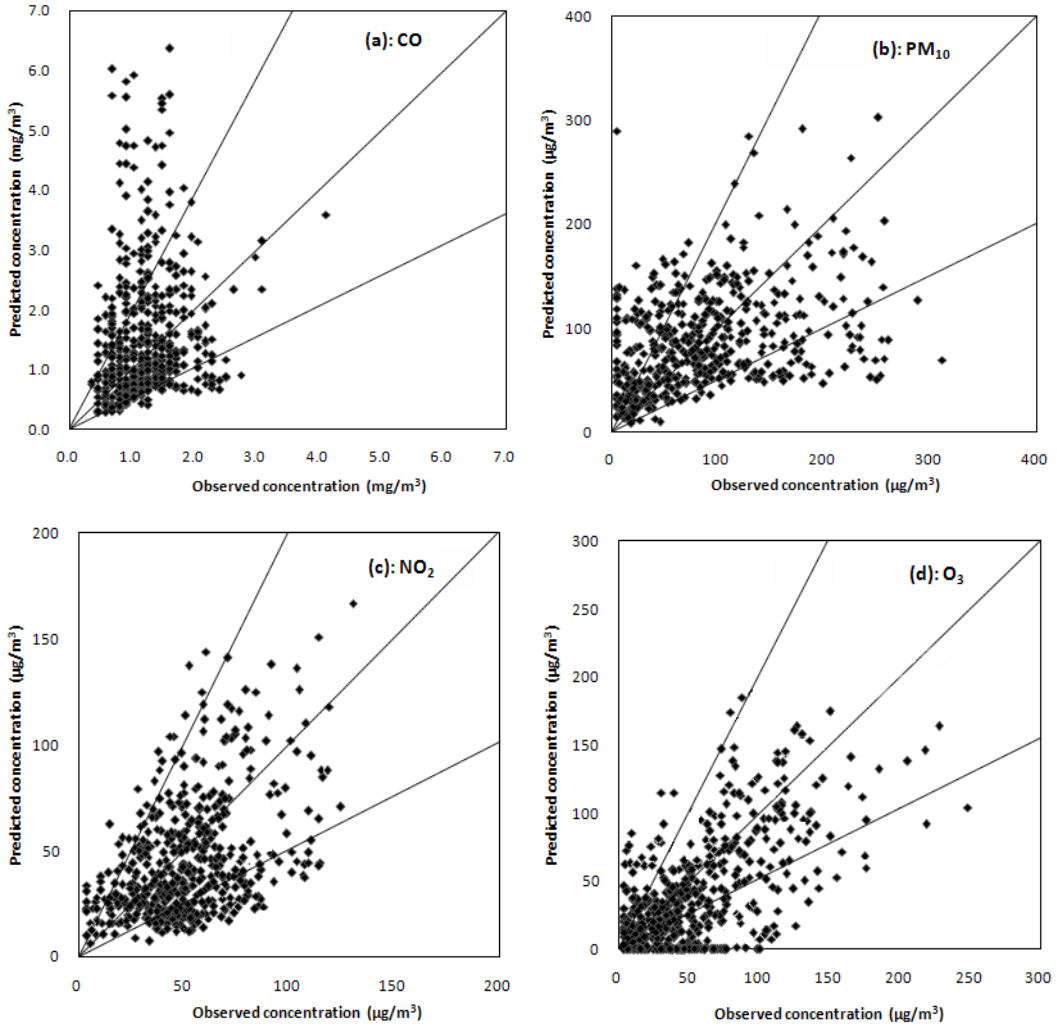

Fig. 3. Scatter plot comparison between observed and predicted hourly concentrations of (a) CO, (b) PM_{10}, (c) NO_2 and (d) O_3 for the periods of July 10^{th}-20^{th} and August 10^{th}-20^{th}, 2008, at the CGZ air quality monitoring site, for the evaluation of ADMS-Urban model. The lines showing an agreement of predictions

and observations by a factor of two are also presented.

Figure 3 (b) and the statistical evaluation reveal that the model predictions of PM_{10} concentrations were very good compared to the observations, rather than an underestimation as some previous field measurements (Okuda et al., 2004; Sun et al., 2004), modelling studies (Song et al., 2006a; Wang et al., 2008a) and source apportionment work (Zheng et al., 2005; Song et al., 2006b; Song et al., 2007; Zhang et al., 2007; Wang et al., 2008b; Xie et al., 2008) would expect. These good PM_{10} predictions in this study were credible, primarily due to the distinct characteristic of source emissions during the Games when a series of control measures were taken for sectors other than on-road vehicles, which were expected to decrease significantly the contributions from soil dust, coal or fossil fuel combustion, industry, secondary sources and biomass burning, the identified major sources for PM_{10} or $PM_{2.5}$ in Beijing by previous work (Okuda et al., 2004; Sun et al., 2004; Zheng et al., 2005; Song et al., 2006a,b; Zhang et al., 2007; Wang et al., 2008b; Xie et al., 2008). Consequently, on-road vehicles became the remaining major source, with relatively more PM_{10} emissions and a higher contribution for PM_{10} during the particular period. Moreover, the PM_{10} or $PM_{2.5}$ samples used for the previous source apportionment studies in Beijing were collected with samplers located at the roofs of several sites, of which the heights ranged from one story (about 5 metres) to five stories (about 25 metres) (Zheng et al., 2005; Song et al., 2006b), and even to 40 metres (Zhang et al., 2007). These PM measurements obtained on the roofs of buildings tended to be less influenced by on-road vehicles of which the exhaust tailpipe height was usually below 0.3 meter. Besides, according to a previous study focusing on the vertical profile of PM near major roads, both the PM_{10} and $PM_{2.5}$ concentrations decreased substantially on the top of a high-rise residential building compared to their ground-level values

514 near roadways (Wu et al., 2002). Therefore, the PM measurements used in the
515 previous source apportionment studies tended to underestimate the PM contribution
516 from on-road vehicles, while on-road vehicles considered in this study had a more
517 substantial impact on the PM_{10} concentrations, which were predicted at a much lower
518 height of 1.5 metres. Furthermore, the background concentrations of PM_{10} from a
519 representative rural monitoring station was added during the modelling, to take into
520 account the contributions from other minor source emissions that were not included
521 specifically in the model run. Thus, the distinct characteristic of source emissions
522 during the particular Olympic period, larger influence of on-road vehicles on
523 predicted PM_{10} concentrations in this study than previous measurements, and the use
524 of background data from a rural monitoring station, resulted in reasonably good
525 predictions compared to the observations, rather than an underestimation of predicted
526 PM_{10}, and the slight overestimation of PM_{10} was therefore not coincidental at the
527 station chosen for model evaluation.

528 3.1.2 Dependence of model performance on time-of-the-day

529 Diurnal profiles on hourly average have been separately plotted for all pollutants
530 measured and predicted at CGZ, as shown by Figure 4. The model captured well the
531 diurnal variations of CO, PM_{10}, NO_2 and O_3, and did particularly well for NO_2 and O_3
532 at predicting the observed peaks. The predicted morning peaks of CO and PM_{10}
533 were about three hours earlier than the observed, but were in good agreement with the
534 morning peak of traffic flows. In addition, the temporal variations of predicted CO
535 and PM_{10} concentrations changed more dramatically than the observed, with a notably
536 overprediction in peak CO concentrations, which was mainly related to an

overestimation of the CO emission factor adopted by the model, resulting in a relatively larger overestimation of emission rates during the rush hours with higher traffic flows than other periods of the day. Moreover, Figure 4 showed that the model had an excellent performance in predicting the diurnal profile of NO_2 and O_3, which revealed the satisfactory model performance in reasonably predicting the temporal variation of secondary gases like NO_2 and O_3 with the application of the GRS chemical scheme. Consequently, the model captured the evening peak NO_2 concentrations, and the afternoon peak ozone concentrations accompanied by the trough NO_2 concentrations.

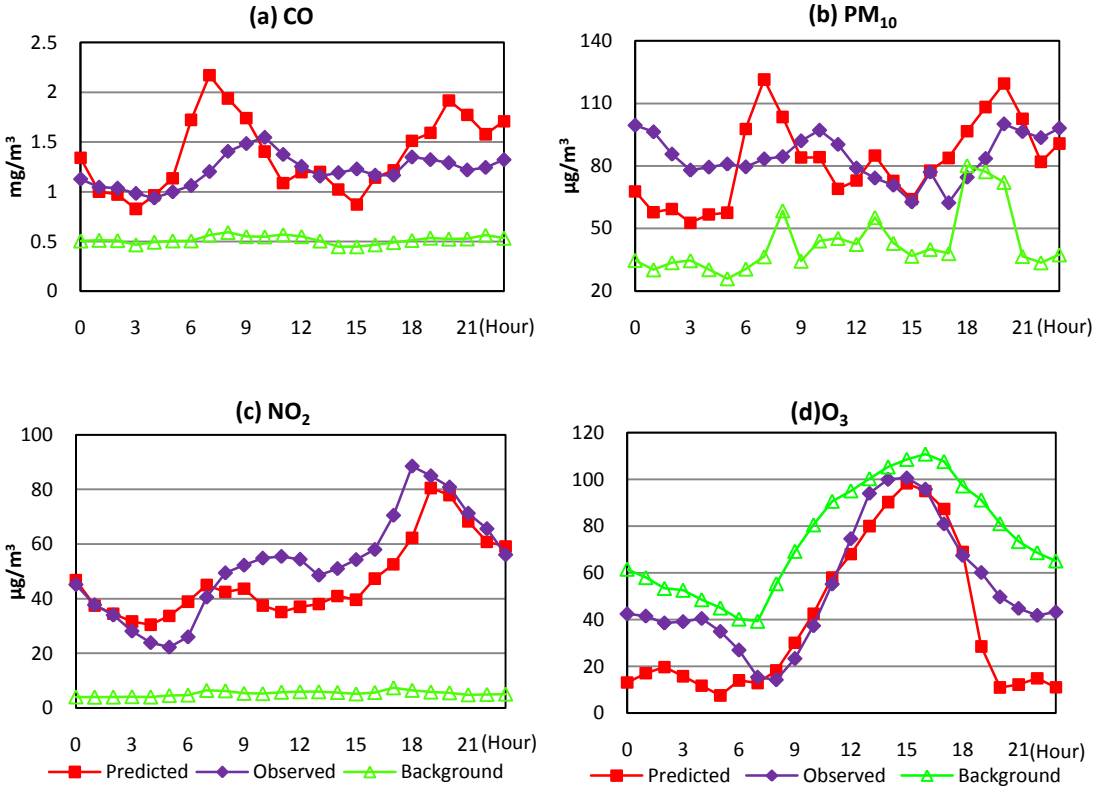

Fig. 4. Model performance on time-of-the-day, in comparison with the diurnal profiles of observed and background concentrations for (a) CO; (b) PM_{10}; (c) NO_2 and (d) O_3, for the periods of July 10^{th}-20^{th} and August 10^{th}-20^{th}, 2008.

551 3.1.3 Dependence of model performance on wind direction

552 Although wind speed has an important influence on the dispersion of pollutant and
553 thus the model predictions of pollutant concentrations, we do not focus on the
554 evaluation of the dependence of model performance on wind speed, because the
555 fundamental factor influencing the diurnal profile of model predictions was the
556 temporal variation of source intensity and subsequent atmospheric chemical reactions,
557 rather than the accompanying wind speed. However, to evaluate the dependence of
558 model performance on wind direction was important to know whether the
559 meteorological station adopted in this study was representative of the wind field of the
560 study domain, and to understand for the right reason the characteristics of spatial
561 distribution of the traffic-related air pollution after the TRS was implemented. Thus,
562 the pollution roses for all pollutants were plotted, as showed by Figure 5, which
563 revealed that the peaks and troughs of the predicted and observed concentrations were
564 virtually in the same directions. This proved that the model well predicted the
565 variance of concentrations in response to the wind direction variation. Besides,
566 Figure 5 also revealed that there was a clear dependence of concentrations on wind
567 directions for all pollutants: high CO concentrations occurred mainly in the downwind
568 southwesterly, northwesterly and southerly directions, with high PM_{10} concentrations
569 also occurring in the downwind southwesterly and northwesterly directions. In
570 addition, NO_2 concentration had a weaker dependence on wind directions and
571 distributed more uniformly in each direction, with the peak concentrations mainly

572 occurring in the southwesterly direction. O_3 had a very clear dependence of wind
573 direction, with the peak concentrations appearing in the northwesterly and
574 southwesterly directions. Therefore, the model captured well the spatial variation of
575 the pollutant concentrations in response to the wind direction variation, which
576 revealed that the meteorological data from the Airport Meteorological Observatory
577 were well representative of the wind field of UAB, in consistence with another study
578 using the same meteorological data source for the evaluation of air quality impacts of
579 the Games (Wang et al., 2009a).

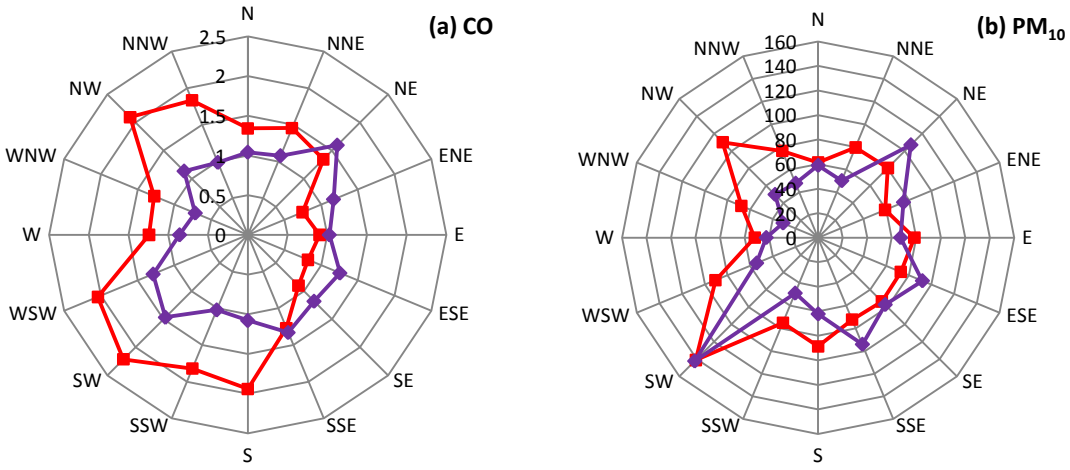

580

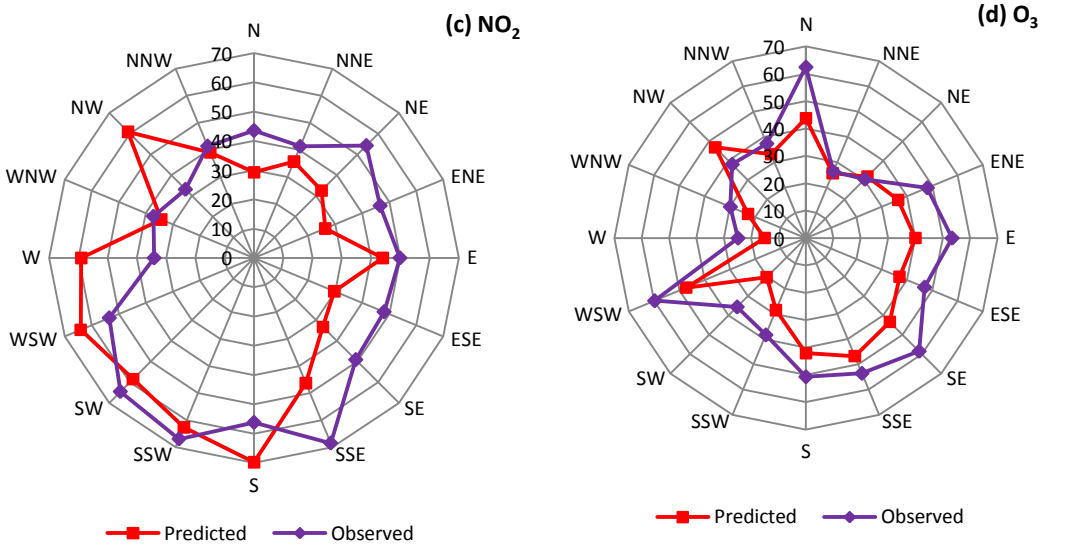

581

582 Fig. 5. Comparison of mean predicted and observed pollutant concentration roses for
583 (a) CO, (b) PM_{10}, (c) NO_2 and (d) O_3 in different wind directions for the periods of
584 July 10^{th}-20^{th} and August 10^{th}-20^{th}, 2008, at the CGZ air quality monitoring site.
585 Only one traffic-representative monitoring station was included in the model
586 evaluation, because the data from the other one, the Qianmen station set up at a
587 high-traffic environment and maintained by the Beijing Municipal Environmental
588 Monitoring Centre (BMEMC), were incomplete during the evaluation period, with
589 about 70% of the data missing due to malfunction of the monitoring equipment.
590 Besides, as industrial production were restricted, construction sites were shut down,
591 and agricultural activities, particularly biomass burning in rural areas were strictly
592 banned both in Beijing and other eight surrounding provinces (MEP, 2008), the major
593 emissions in the UAB during the Games came from vehicles, and this emission
594 characteristic during the Games was distinct from the usual situation with much more
595 emissions from other sources, under which circumstances the previous modelling
596 studies (Song et al., 2006b and Wang et al., 2008a) were conducted, using additional
597 rural and industrial monitoring stations for the modelling evaluation. Therefore, the
598 overall good model evaluation results in this study based on the CGZ monitoring
599 station were not coincidental due to the station location, but was a true reflection of
600 the particular characteristic of source emissions dominated by vehicles during the
601 Games. Under such a circumstance, a city-level evaluation of the model
602 performance was not conducted in this study, as the particular characteristic of
603 sources emissions during the Games convinced us that other air quality monitoring
604 stations, particularly those usually adopted to reflect air quality impacts from
605 industrial sources or rural emissions, were unnecessary or not suitable to be included
606 for the model evaluation in this study. Furthermore, since the following analysis of

607 the modelling results was focused on the predictions at the simulated roads and at the
608 receptors, where the traffic-dominant emission characteristic was identified and the air
609 quality responses have been evaluated, using the measurements from the
610 representative traffic monitoring station (CGZ), it is reasonable to believe that the
611 conclusions drawn based on the analysis were credible. Nevertheless, the possible
612 drawback of using one traffic-representative station for model evaluation was that the
613 model predictions in areas away from the simulated roads might have some unknown
614 uncertainty.

615 3.2 Air quality impacts in response to TRS policy before, during and after the Games

616 Applying the evaluated ADMS model, we predicted the CO, PM_{10}, NO_2 and O_3
617 concentrations from the RRs and LRs around UAB before, during and after the
618 Olympic Games, with the aim of evaluating the air quality impacts of the TRS policy.
619 First, the emission reduction in accordance with the decrease of traffic flows was
620 reported; Second, the daily and diurnal variation of pollutant concentrations along the
621 RRs and LRs were compared for the pre-, during- and post-TRS periods, followed by
622 a further assessment of the weekly variation of air quality in response to the TRS
623 policy; Finally, the spatial variation of the traffic-related air pollution for the pre-,
624 during- and post-TRS periods was assessed, to understand the regional differences in
625 air quality impacts of the TRS policy.

626 3.2.1 Reduction of diurnal average traffic flow and pollutant emissions

627 The traffic flows on the RRs and LRs had a notable reduction after the TRS policy
628 was implemented on 20th July, 2008. The daily average traffic flows of the short and

long motor vehicles for the during-TRS period had a reduction of 26.1% and 11.0%, respectively, compared to the pre-TRS period. Figure 6, which shows the variation of traffic flows on RRs and LRs on daily average and the variation of the diurnal profiles of the total traffic flow on hourly average for the pre-TRS, during-TRS and post-TRS periods, revealed that the TRS policy had a substantial effect on the reduction of both daily average and hourly average traffic flows, with average reduction rates of 22.4%, 26.1%, 27.7% and 27.6% on the 2nd, 3rd, 4th RR and the LRs, respectively, and a notably overall reduction of about 26.1% for the total traffic flow. Particularly, the TRS policy had a largest traffic flow reduction of 30.8% during the morning rush hours (7-8 am). On the other hand, both the daily average and hourly average traffic flows on all types of roads during the post-TRS period virtually bounced to the same level as the pre-TRS period, with the double-peak pattern of the diurnal profile of traffic flows in Beijing unchanged by the TRS policy.

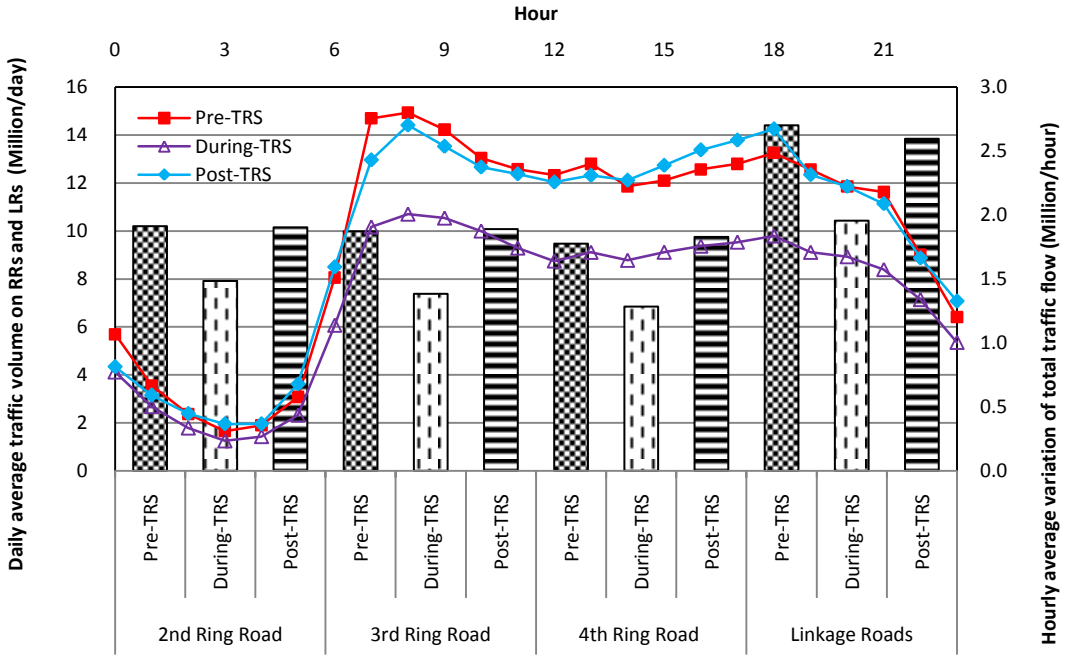

643 Fig.6. Comparison of traffic flows on 2nd RR, 3rd RR, 4th RR and the LRs on daily
644 average (histograms), and diurnal variation of total traffic flow on hourly average
645 (scatter plots) for the pre-TRS, during-TRS and post-TRS periods, respectively.

646 With the reduction of traffic flows, the traffic conditions were improved and the
647 traffic running speeds on hourly average increased by about 15% for the during-TRS
648 period, as revealed by the ITS-TAP monitoring network. The raised speed decreased
649 the emission factors of CO, PM_{10} and NO_x for all vehicle types, as calculated by
650 COPERT model. In addition to the reductions of traffic flows and emission factors,
651 the emissions on daily average decreased by about 26.1%, 25.4% and 25.2% for CO,
652 PM_{10} and NO_x, respectively. Consequently, emission rates on the RRs and LRs
653 decreased as well, especially for the 3rd, 4th RR and the LRs.

654 3.2.2 Temporal variation of air quality impacts of the TRS policy
655 Pollutant concentration levels are directly related to air quality, and thus we focused
656 on the pollutant concentration impacts of the TRS policy to assess its effectiveness on
657 air quality improvement in Beijing during the Games. Concentrations of CO, PM_{10},
658 NO_2 and O_3 in the following results and discussion were predicted at a height of 1.5
659 meters above the ground.

660 3.2.2.1 Changes in daily average concentrations for the pre-, during- and post-TRS
661 periods

662 The daily average concentrations of CO, PM_{10}, NO_2 and O_3 had a notable reduction
663 on the RRs and LRs around UAB after the TRS policy was implemented, as shown by
664 Figure 7, which illustrates that the daily average predictions of CO, PM_{10}, NO_2 and O_3

665 on the 2nd, 3rd, 4th RR and the LRs for the pre-, during- and post-TRS periods. Daily
666 average CO concentrations were about 2.1, 2.1, 2.2 and 2.3 mg/m^3 on the 2nd, 3rd, 4th
667 RR and LRs, respectively, for the pre-TRS period, which decreased by about 35.8%,
668 38.5%, 34.9% and 35.6% on the 2nd, 3rd, 4th RR and LRs, respectively, for the
669 during-TRS period. Consequently, the CO daily concentrations on all road types
670 satisfied the CNAAQS Grade II of 4 mg/m^3 for the during-TRS period. The
671 pre-TRS daily average concentrations of PM_{10} were 120.9, 115.7, 136.1 and 163.2
672 μg/m^3 on the 2nd, 3rd, 4th RR and the LRs, respectively, which was successfully
673 reduced below 150 μg/m^3 by the TRS policy, as shown by Figure 7. For the
674 pre-TRS period, 40% of days on the LRs exceeded the daily CNAAQS Grade II of
675 150 μg/m^3, while the PM_{10} daily concentrations on the LRs were successfully reduced
676 by 34.7%, to satisfy the Grade II limit, with the PM_{10} concentrations on the 2nd, 3rd
677 and 4th RR reduced by 38.7%, 31.8% and 44.0%, respectively, resulting in satisfaction
678 of the Grade II limit for every single day for the during-TRS period. The reduction
679 of vehicular emissions of PM_{10} due to the TRS policy, which was the major cause for
680 PM_{10} emission reduction during the Games, as control measures for sources other
681 than on-road vehicles remained unchanged and had little extra effect on emission
682 reduction, resulted in this reasonably notable effect on the reduction of PM_{10}
683 concentration, which the previous source apportionment studies would not expect.
684 With the bounce of traffic flows during the post-TRS period, concentrations of both
685 CO and PM_{10} increased notably, with 20% of days on the LRs exceeds the Grade II

686 limit for PM_{10}. The NO_2 concentrations were reduced by about 30.3%, 31.9%, 32.3%
687 and 33.9% on the 2nd, 3rd, 4th RR and the LRs, respectively, to about 52.3, 46.2, 45.9
688 and 47.0 μg/m^3 during the TRS period, with the daily concentration on every single
689 day during this period conforming to the CNAAQS Grade II of 80 μg/m^3. Only 10%
690 of days on the 2nd RR exceeded the NO_2 Grade II limit for the post-TRS period,
691 despite a concentration increase of about 9.0%, 13.7%, 17.3% and 18.8% on the 2nd,
692 3rd, 4th RR and the LRs, respectively, during the period. O_3, of which the
693 concentration level is usually lower in the source-intensive urban areas than in the
694 rural areas, had a concentration of about 38-52 μg/m^3 in the urban areas during the
695 pre-TRS period, and the O_3 concentration decreased to about 24-29 μg/m^3 during the
696 TRS period, which was consistent with the findings of Wang et al. (2009b). Unlike
697 other pollutants, the O_3 concentration continued decreasing for the post-TRS period,
698 to about 23-26 μg/m^3 despite the increase of traffic flow and vehicular emissions.
699 This is mainly because O_3 concentrations in UAB are produced by local
700 photochemical reactions under VOC-limited conditions (Wang and Li, 2002; Wang et
701 al., 2009c), and higher emission level of NO during the post-TRS period consumed O_3
702 and suppressed the accumulation of O_3 in urban environment of Beijing (named the
703 "titration effect") (Chou et al., 2006; Sadanaga et al., 2008). Besides, the elevated
704 nitrogen dioxide (NO_2) through the titration effect and reactions of NO with other
705 radicals further reacted with the OH radical and yielded nitric acid (HNO_3), which
706 ended the photochemical reaction chain involved with the OH radical that otherwise

accumulates the ambient O_3 concentration (NARSTO, 2000). Therefore, it was clear that the TRS policy was effective in reducing daily average concentrations of pollutants, ensuring that the air quality in Beijing during the Olympic Games conformed to the 24 hours CNAAQS Grade II limits.

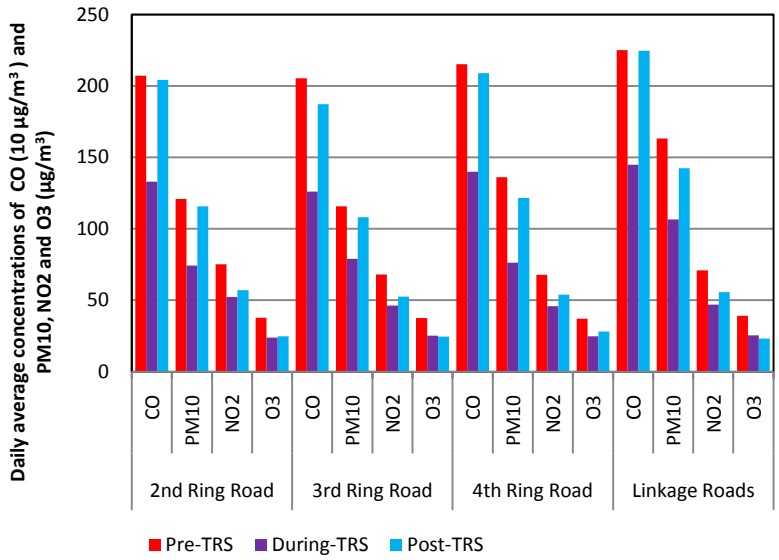

Fig. 7. Comparison of daily average predicted concentrations of CO, PM_{10}, NO_2 and O_3 on different road types for the pre-TRS, during-TRS and post-TRS periods.

The predicted highest daily average concentrations of the CO, PM_{10}, NO_2 and O_3, which occurred at a very limited area under certain circumstances, also showed a notable decrease during the TRS period, which was in consistence with the previous study proving the effectiveness in reducing extreme concentrations of a four-day traffic control experiment by the Beijing Municipal Government (Westerdahl et al., 2009). The predicted highest concentrations had decreased from 6.3 to 4.6 mg/m^3 for CO, from 635.7 to 498.3 $\mu g/m^3$ for PM_{10}, from 194.7 to 154.2 $\mu g/m^3$ for NO_2 and from 88.2 to 53.3 $\mu g/m^3$ for O_3, a reduction of about 27.6%, 21.6%, 20.8% and 39.6%

722 for CO, PM_{10}, NO_2 and O_3, respectively, in comparison with the pre-TRS period.

723 3.2.2.2 Diurnal variation of hourly average concentration

724 To further evaluate the effectiveness of the TRS policy on air quality improvement,
725 we focused on the variation of diurnal profiles of hourly average concentration on the
726 RRs and LRs in response to the TRS policy. Figure 8 shows that hourly average
727 concentrations of CO, PM_{10}, NO_2 and O_3 on the RRs and the LRs decreased notably,
728 in comparison with the pre-TRS period. The morning and evening peak
729 concentrations of CO on the LRs had decreased from about 3.29 mg/m^3 to about 1.83
730 mg/m^3, the largest reduction of 34.9% and 38.0% among all road types, as shown by
731 Figure 8 (a), while the largest reduction of the morning and evening peak
732 concentrations of PM_{10} was observed on the 2nd RR, accounting for about 37.8% and
733 40.2%, respectively. Consequently, the hourly CO concentrations were well below
734 the 1-hour CNAAQS Grade II of 10 mg/m^3 and the hourly PM_{10} concentrations
735 decreased below 150 $\mu g/m^3$ on all types of roads. Particularly, the average of
736 evening peak CO, PM_{10} and NO_2 concentrations were reduced significantly, by about
737 36.6%, 36.1% and 32.8%, respectively, which was a solid proof for the air quality
738 improvement during the TRS policy period.

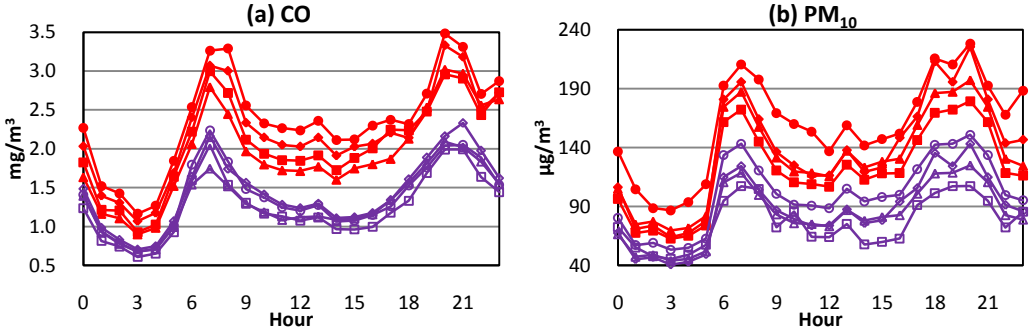

739

740

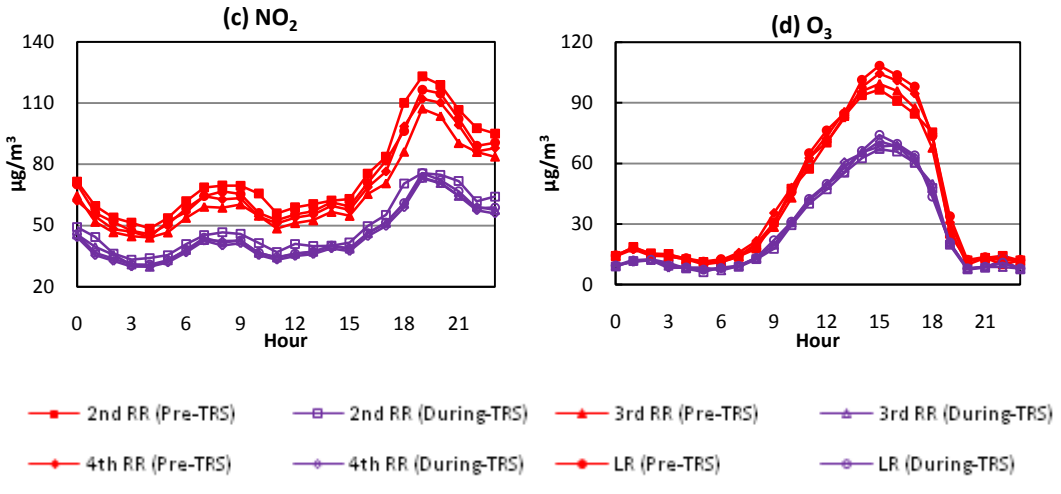

741

742 Fig. 8. Comparison of diurnal predicted variations of hourly concentrations of (a) CO;
743 (b) PM_{10}; (c) NO_2 and (d) O_3 on 2^{nd}, 3^{rd}, 4^{th} RR and the LRs for the pre- and during-
744 TRS periods.

745 For both pre- and during-TRS periods, the diurnal profile of CO and PM_{10} took on
746 an obvious double-peak mode, as shown by Figure 8 (a) and (b), with the morning
747 and evening peak concentrations occurring at around 7-8 am and around 8-9 pm,
748 respectively, and the lowest concentrations occurring at around 3 am. While the
749 occurring time of the morning peak concentration was consistent with the morning
750 rush hour of traffic flows, the evening peaks for CO and PM_{10} were about two to three
751 hours later than the evening rush hour. Moreover, the evening peak concentrations
752 of CO and PM_{10} during the pre-TRS period even exceeded the morning peak, which
753 was in contradiction with the diurnal profile of traffic flows during the period.
754 These delayed and higher evening peak concentrations should be ascribed to the
755 particular evening meteorological conditions in UAB: urban heat island (UHI)
756 frequently occurs in Beijing in the summer night, which tends to produce strong

757 temperature inversion and higher inversion layer at night. When the UHI occurred,
758 the UHI convergence and the strong temperature inversion at night hindered air
759 dispersion and contributed to the local accumulation of pollutants, resulting in high
760 pollution concentrations at night (Miao et al., 2008; Liu et al., 2006).

761 The NO_2 concentrations on all roads for the pre-TRS periods, as shown by Figure
762 8 (c), began to increase in the early morning, reached a peak in about 7-8 am, and
763 came to a trough during the mid-day time, which was related to the traffic and
764 emission rate cycles and similar diurnal variation of NO_2 concentrations were found
765 in the urban area of Cairo (Khoder, 2009). The maximum concentration of NO_2
766 occurred at about 7-8 pm, which was higher in magnitude than the morning peak.
767 This was partly due to the evening rush hour of traffic with high emission rate of NO_x,
768 and partly due to the same UHI effect weakening the dispersion conditions and
769 resulting in evening peak concentrations of CO and PM_{10}. Moreover, the lower
770 temperature and solar radiation intensity in the evening decreased the
771 photodissociation of NO_2, a major chemical mechanism for NO_2 loss during the
772 daytime. The TRS policy, as shown by Figure 8(c), did not alter the diurnal
773 variation characteristic of NO_2 concentrations, but significantly reduced the hourly
774 sequential concentrations of NO_2 during the Games. Particularly, the highest hourly
775 average concentrations of 123.1, 107.2, 111.9 and 116.6 $\mu g/m^3$ on the 2^{nd}, 3^{rd}, 4^{th} RR
776 and the LRs, respectively, which occurred at about 7 pm during the pre-TRS period,
777 were significantly reduced by as much as 38.6%, 31.5%, 34.7% and 32.5%,

778 respectively, to 77.5, 73.4, 73.1 and 75.7 μg/m^3, respectively, during the TRS period,
779 which was in good agreement with the tropospheric NO_2 observations by NASA's
780 OMI revealing a 30-50% reduction of NO_2 during the Games (NASA, 2009).
781 Therefore, the TRS policy was effective in reducing the hourly NO_2 concentrations,
782 and consequently the hourly concentrations on all types of roads were far below the
783 1-hour CNAAQS Grade II of 120 μg/m^3 during the TRS period. As shown by
784 Figure 8 (d), the O_3 concentrations on all roads had a similar diurnal profile for both
785 pre- and during-TRS periods, with the concentrations increasing in the daytime,
786 reaching the peak at about 3 pm and beginning to decrease rapidly. It was clear that
787 the TRS policy reduced remarkably the hourly O_3 concentrations on all types of roads,
788 and had a notable concentration reduction of the afternoon peak, with the
789 concentrations on the 2nd, 3rd, 4th RR and the LRs decreasing by about 35.4%, 30.7%,
790 32.2% and 31.8%, respectively. As a result, the hourly O_3 concentration during the
791 TRS period was far below the 1-hour CNAAQS Grade II of 160 μg/m^3. Meanwhile,
792 it was interesting to find that the diurnal variation of the concentration ratio of NO_2 to
793 O_3 ($[NO_2]/[O_3]$) for all types of roads was opposite to the diurnal profile of O_3
794 concentrations, which revealed that the traffic-related NO_x (mostly NO) consumed O_3,
795 and resulted in an increase of the secondary NO_2 concentration and a decrease of the
796 O_3 concentration, a typical VOC-limited characteristic for ozone formation. With
797 the significant reduction of both primary and secondary pollutant concentration levels,
798 air quality in UAB had therefore been improved remarkably during the Games in

799 response to the TRS policy.

800 3.2.2.3 Weekly variation of diurnal profile of pollutant concentrations for the pre-,
801 during- and post-TRS periods

802 To investigate the day-of-the-week variation of air quality impact in response to the
803 TRS policy, we plotted the diurnal profiles of CO, PM_{10}, NO_2 and O_3 for weekdays,
804 Saturdays and Sundays for the separate periods before, during and after the TRS
805 policy. As shown by Figure 9 (a) and (b), the diurnal profiles for CO and PM_{10}
806 remained similar, with a typical two-peak pattern, and had no obvious weekly
807 variation in response to the TRS policy, as the occurring time of the peaks and trough
808 were consistent for weekdays, Saturdays and Sundays for the three separate periods,
809 due to the smooth weekly cycle of diurnal variation of traffic flows. Notably lower
810 levels of CO and PM_{10} concentrations on Saturdays and Sundays than weekdays,
811 however, were observed, particularly during the rush hours when peak concentrations
812 occurred, for the pre-, during- and post-TRS periods. Therefore, it was clear that the
813 traffic-related air pollution still presented a typical two-peak diurnal variation pattern,
814 but the weekly cycle had no obvious variation in response to the TRS policy, which
815 was, nevertheless, effective in reducing the hourly concentrations, particularly the
816 peak concentrations of CO and PM_{10}.

817 The day-of-the-week variation of NO_2 diurnal profile, as shown by Figure 9 (c),
818 revealed a similarity in the diurnal variation on weekdays, Saturdays and Sundays,
819 particularly, in the ascending trend of NO_2 concentrations in the daytime and reaching

820 a peak in the evening, despite a notable decrease in the afternoon, for the pre-, during-
821 and post-TRS periods. Besides, lower concentration levels on Saturdays and
822 Sundays were observed compared to that on weekdays, which revealed that the TRS
823 policy did not change the weekly cycle of traffic flows, with heavier traffic load on
824 weekdays than on the weekends. Meanwhile, Figure 9 (d) revealed a notable
825 difference between the diurnal profile of O_3 and other pollutants, with relatively
826 higher concentration levels on Saturdays and Sundays than that on weekdays for the
827 pre- and post-TRS periods, which was in agreement with the characteristic of the
828 ozone weekend effect that has been frequently observed in urban areas
829 (Atkinson-Palombo et al., 2006; Gao and Niemeier, 2007; Murphy et al., 2007; Tang
830 et al., 2008; Khoder, 2009). The major reason for the observed ozone weekend
831 effect was the "VOC-limited" feature for ozone formation in UAB: the ozone
832 concentration tended to increase with the decrease of NO_x emissions, typically due to
833 the reduction of traffic flows, as a result of the weakened titration effect of lower NO_x
834 emissions on the weekends that tended to accumulate ozone concentrations. This
835 mechanism also explained why a more remarkable ozone weekend effect was
836 observed for the post-TRS period, as shown by Figure 9 (d): the peak O_3
837 concentration at around 3 pm on weekdays for the post-TRS period continued to
838 decrease, compared to the during-TRS period, due to the enhanced titration effect of
839 increased NO_x emissions that suppressed the ozone formation on weekdays, while the
840 peak concentrations on Saturdays and Sundays increased, due to a larger reduction of

841 NO_x emissions and thus a more weakened titration effect on the weekends during the
842 post-TRS period, compared to the during-TRS period. Moreover, Figure 9 (d) also
843 revealed that the TRS policy effectively reduced both the hourly peak and daily
844 average concentrations of ozone, and meanwhile reduced and virtually removed the
845 weekend effect of ozone for the during-TRS period, probably due to the smoother
846 weekly variation of traffic flows resulting from the restriction on traffic.
847

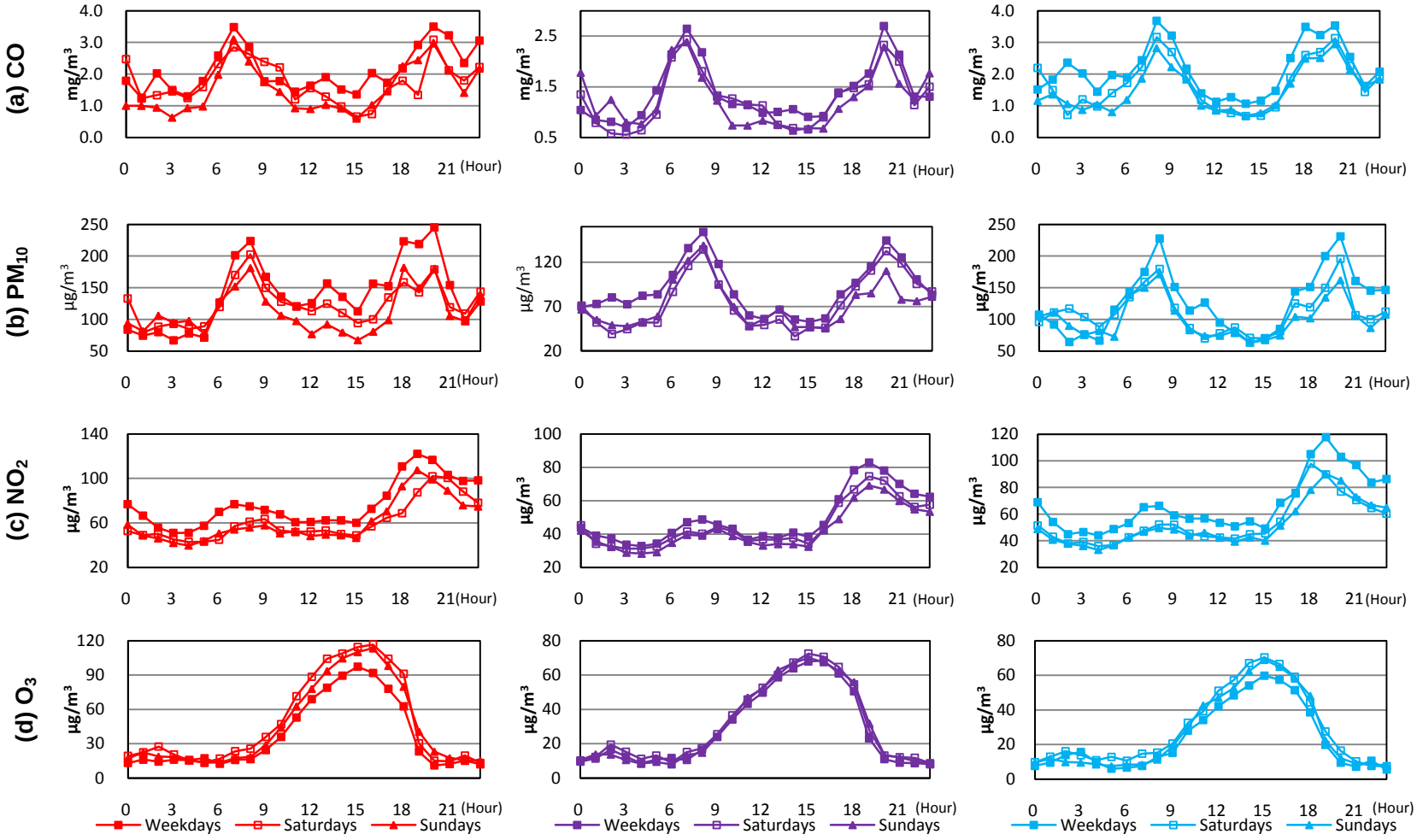

Fig. 9. Day-of-the-week variations of (a) CO; (b) PM_{10}; (c) NO_2 and (d) O_3 diurnal profiles in response to the implementation of the TRS policy.

847 3.2.3 Spatial variation of traffic-related air pollution and implication on regional air
848 quality improvement for the pre-, during- and post-TRS periods
849 To investigate the regional air quality impacts of the TRS policy, we looked into the
850 spatial distribution of the traffic-related air pollution around UAB, as well as the
851 spatial variation of regional air quality improvement in response to the TRS policy.
852 Figure 10, which illustrates the contour plot of the daily average concentrations of
853 CO, PM_{10}, NO_2 and O_3 from on-road motor vehicles on the 2^{nd}, 3^{rd}, 4^{th} RR and the
854 LRs, for the pre-, during- and post-TRS periods, respectively, revealed remarkable
855 differences in the regional distribution of traffic-related air pollutant concentrations
856 and notable variation of regional air quality in response to the TRS policy. Before
857 the TRS policy was placed, the highest and lowest CO concentration levels occurred
858 in the upwind eastern regions and the southern areas, respectively, as shown by
859 Figure 10 (a), with the daily average concentrations of the representative receptors
860 located in the downwind northwest and upwind southeast accounting for about 2.56
861 and 2.02 mg/m^3, respectively. Particularly, the West 2^{nd} RR and the Northwestern
862 LRs between 2^{nd}, 3^{rd} and 4^{th} RR had the heaviest traffic and accordingly suffered the
863 highest CO concentration level of above 2.4 mg/m^3. With the TRS policy, a
864 significant reduction of the CO daily average concentration was achieved, and the
865 previously highest concentration in the north was reduced by 31.2%, to 1.79 mg/m^3,
866 with the concentration levels in the south, west and east regions decreasing by about
867 17.6%, 18.2% and 17.6%, respectively. Besides, CO concentrations in a broad area

868 of the northeast, east and southeast outside the 4th RR decreased below a level of 0.5
869 mg/m^3, mainly due to the prevailing northeast, east and southeast wind that
870 transported the pollutant to the downwind directions and resulted in a relatively
871 lower concentrations in these upwind areas during the period. Moreover, the
872 previously seriously polluted areas in the West 2nd RR and the Northwestern LRs
873 were relieved, with a much smaller area where the concentration level remained
874 above 2 mg/m^3. Therefore, the TRS policy was effective in bringing down the
875 concentration levels in both the most polluted areas and different parts of the urban
876 area, resulting in a much better air quality during the Games. With the bouncing of
877 traffic flows almost to the pre-TRS level, the CO concentration increased
878 dramatically in every part of UAB, and consequently, almost caught up with the
879 previous level before the TRS policy was placed, with the concentrations in the east,
880 south, west and north increasing by about 24.2%, 16.0%, 15.2% and 22.2%,
881 respectively.

882 The spatial distribution of PM_{10} concentrations was characterized as linear
883 distribution of relatively higher pollution along the RR and the LRs, with
884 concentration levels in the areas between the simulated roads and outside the 4th RR
885 much lower. For the during-TRS period, the PM_{10} concentration levels decreased
886 remarkably for the whole UAB, with the PM_{10} concentration in most of the area
887 reduced below 100 μg/m^3. Particularly, the previously highly polluted areas in the
888 West 2nd RR, Southwestern 4th RR and the Northern LRs with PM_{10} concentrations

above 150 μg/m^3 before the TRS shrank significantly during the TRS, as shown by Figure 10 (b). Consequently, the concentrations in the east, south, west and north regions of UAB decreased from about 118.2, 111.9, 160.4 and 217.7 μg/m^3, respectively, for the pre-TRS period, to about 66.1, 67.6, 105.6 and 155.2 μg/m^3, respectively, for the during-TRS period. The dramatically decrease of the primary pollutant concentration indicated that the air quality during the Games was improved significant in response to the TRS policy. However, the PM_{10} concentration levels increased by about 23.4%, 33.6%, 20.7% and 29.5%, respectively, in the east, south, west and north regions for the post-TRS period. As a result, the areas with PM_{10} concentration above 150 μg/m^3 expanded, which proved reversely the effectiveness of the TRS policy on air quality improvement.

The spatial distribution of NO_2 concentration was more influenced by the prevailing northeasterly, easterly and southeasterly winds during the pre-TRS period, with the relatively higher daily average concentration of about 76.8 and 68.0 μg/m^3 predicted in the downwind western areas and the northern traffic-heavy areas, respectively. Besides, the daily average NO_2 concentration along the West 2nd RR, the Northern LRs and part of the West 4th RR exceeded the CNAAQS Grade II of 80 μg/m^3. On the contrast, the NO_2 concentration decreased significantly in response to the TRS period, with the concentration level in most of UAB below 80 μg/m^3, which was a clear evidence of the effective control of traffic-related air pollution and corresponding remarkable air quality improvement by the TRS policy. Particularly,

910 better effect on pollution reduction was observed in the previously most severely
911 polluted areas, as the concentration level in these areas were brought down
912 sufficiently to comply with the CNAAQS limited values. With the expiration of the
913 TRS policy, NO_2 pollution with concentration above 80 and even 120 μg/m^3
914 appeared in a much larger area for the post-TRS period, and NO_2 concentration
915 increased significantly in the downwind western areas, in comparison with the
916 during-TRS period, as shown by Figure 10 (c). The spatial distribution variation of
917 NO_2 concentration in UAB revealed a notable air quality improvement due to
918 reduced on-road vehicular emissions.

919 The spatial distribution of O_3 concentration was distinct from those of CO, PM_{10}
920 and NO_2, as shown by Figure 10 (d). For the pre-, during- and post-TRS periods,
921 notably lower O_3 concentrations were observed along the RR and the LRs as these
922 areas were the emission sources and O_3, as a typical secondary air pollutant, had its
923 higher concentration levels in the relatively remote areas off the road sources.
924 Consequently, the O_3 daily average concentration in the near-road areas was well
925 below 60 μg/m^3 for the pre-TRS period and relatively higher concentration levels of
926 60-80 μg/m^3 and above 80 μg/m^3 covered a large area around and outside UAB
927 where no direct vehicular emissions were generated. Particularly, the severely
928 polluted West 2nd RR, Northern LRs and part of the South 4th RR areas with high
929 concentration levels of CO, PM_{10} and NO_2, however, had the lowest O_3
930 concentrations. In response to the TRS policy, the O_3 concentrations in the East,

South, West and North regions of UAB decreased significantly from 43.3, 46.6, 36.4 and 43.9 μg/m^3, respectively, to about 30.7, 31.2, 23.7 and 24.4 μg/m^3, respectively, mostly due to the decrease of the precursor emissions of NO_x and VOC from on-road vehicles. Moreover, the O_3 concentration during the post-TRS period continued to decrease, despite the increase of vehicular emissions of NO_x and VOC. As has been discussed previously, this phenomenon was mostly due to the "VOC-limited" characteristic for ozone formation in UAB. Therefore, the spatial variation of O_3 concentrations in response to the TRS policy also provided solid evidence of the effectiveness of such a restriction policy on air quality improvement during the Games.

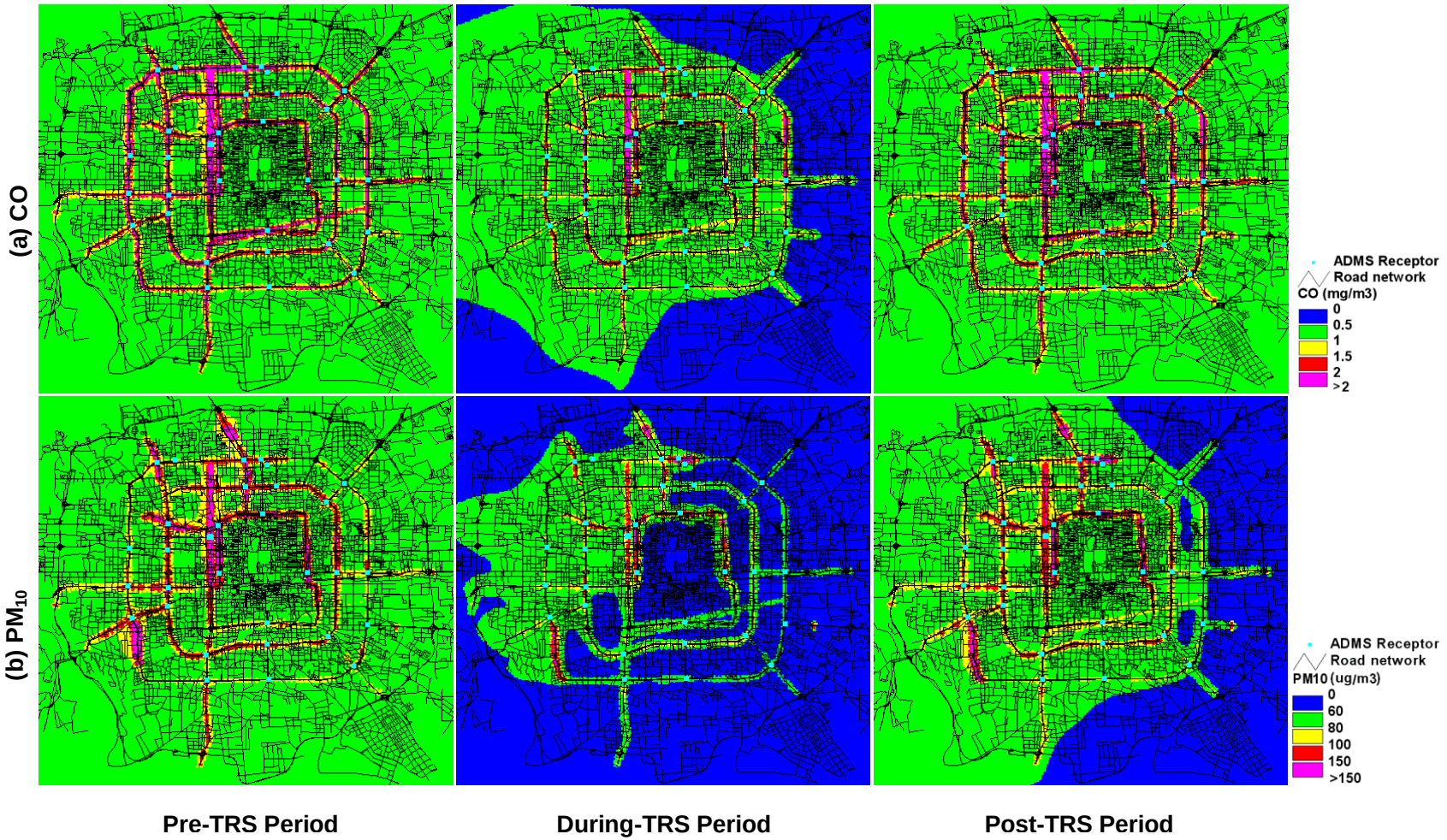
(a) CO
(b) PM10
ADMS Receptor
Road network
CO (mg/m3)
0
0.5
1
1.5
2
>2
ADMS Receptor
Road network
PM10 (ug/m3)
0
60
80
100
150
>150
Pre-TRS Period
During-TRS Period
Post-TRS Period

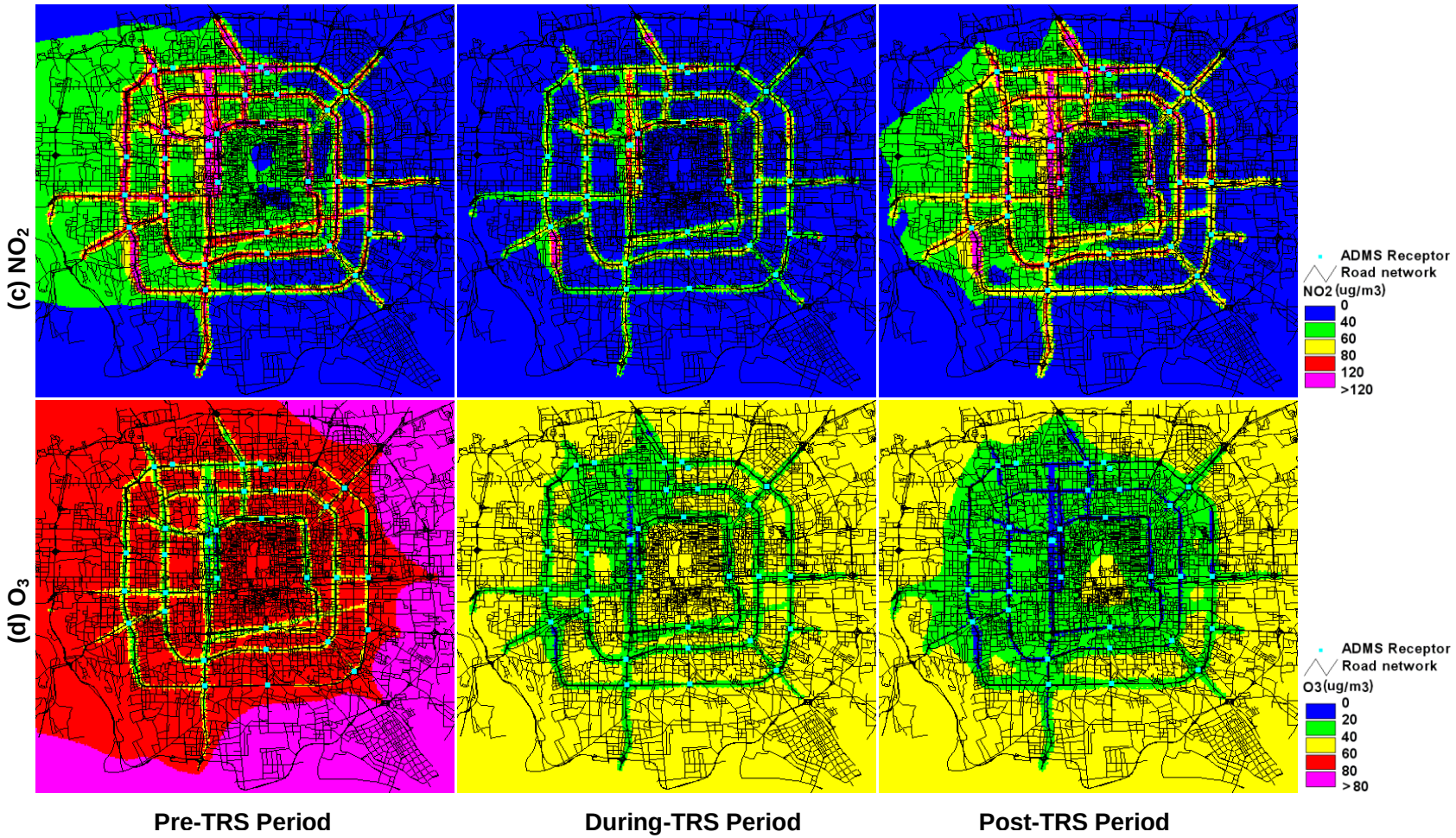

Fig. 10. Spatial distribution of (a) CO; (b) PM_{10}; (c) NO_2 and (d) O_3 concentrations on daily average for pre-, during- and post-TRS periods, and the spatial variation of regional air quality impacts in response to the TRS policy.

941 3.3 Contribution of traffic flow reduction, raise of running speed and meteorological
942 conditions to air quality improvements during the TRS period
943 It is meaningful to understand deeply the reasons that resulted in the air quality
944 improvement after the TRS policy was implemented, to make sure that the model
945 performed well for the right reasons, and to learn and inherit the useful experiences
946 for the future air quality management in Beijing and other cities of China. Therefore,
947 we focused on a discussion about the air quality impacts of traffic flow reduction,
948 raise of running speed, variation of emission factors of pollutants, as well as the
949 meteorological condition variation during the Games.
950 The TRS policy had a direct impact on the traffic flow and the running speeds of
951 traffic fleet. As revealed by the ITS-TAP system, the daily average traffic flows of
952 short and long vehicles during the TRS period decreased by 26.1% and 11.0%,
953 respectively, an average reduction of about 24.2% for the total traffic fleet, in
954 comparison with the pre-TRS period. Besides, running speed on the 2^{nd}, 3^{rd}, 4^{th} RR
955 and the LRs increased by 18.5%, 12.8%, 15.3% and 13.8%, respectively, an average
956 15% increase in driving speeds of total traffic fleet, estimated based on the fractions
957 of traffic flows on these roads after the TRS policy took effect, which had a positive
958 effect on reducing emission factors of pollutants. Figure 11 (a) illustrates the
959 decrease rates of model-calculated emission factors of CO, PM_{10} and NO_x from
960 various vehicle types resulting from the raise of running speed. The PC and LDV,
961 which were mostly gasoline vehicles, had the largest reduction of CO emission factor,

962 accounting for about 10%. The largest reductions of both NO_x and PM_{10} emission
963 factors were ascribed to diesel HDV, of which the traffic flow accounted for only 1-2%
964 of the total fleet. Therefore, the reduction of NO_x emission factor mainly relied on
965 the other vehicle types, and an overall 3% reduction in NO_x emission factor was
966 achieved. The PM_{10} emission factors were assumed constant for gasoline PC and
967 LDV in response to the running speed increase, as there were no domestic studies
968 available reporting the variation of PM emission factors of gasoline vehicles induced
969 by speed raise, like from 20 km/h to 23 km/h, and a comprehensive sensitivity
970 evaluation of the USEPA's MOBILE 6.2 model for PM emission factor found that a
971 speed increase from 20 km/h to 23 km/h had very little impact on PM emission factor
972 and concluded that speed has a negligible effect on PM emission factors for gasoline
973 vehicles, which was unlike the emission factors for CO NO_x and VOC that were
974 highly sensitive to speed (Granell et al., 2004), while the HDV and buses had a
975 reduction of about 10% of PM_{10} emission factor. Consequently, the emissions of CO,
976 PM_{10} and NO_x were reduced by about 26.1%, 25.4% and 25.2%, respectively, and the
977 daily average concentrations of CO, PM_{10}, NO_2 and O_3 decreased by about 25.5%,
978 35.4%, 32.1% and 34.4%, respectively, in response to the TRS policy. Therefore,
979 the TRS policy was effective in bringing down traffic-related emissions, by a
980 dominant contribution of traffic flow reduction, and by an extra bonus of decreasing
981 emission factors due to the improvement of driving conditions. Taking into account
982 the variation of wind speed, a major meteorological factor that affected the

traffic-related air pollution, the daily average wind speeds were about 2.52 and 2.53 m/s for the pre- and during-TRS periods, respectively, and had no statistically significant difference ($p<0.05$). Besides, the diurnal wind speed profile on the hourly average had little variation, particularly in the morning and for the evening rush hours (7-8 pm), as shown by Figure 11 (b). Under the virtually constant wind speed, the TRS policy turned out an effective measure in simultaneously bringing down traffic flow, increasing traffic fluency, and achieving air quality improvement with significantly decreased concentration levels. Therefore, the TRS policy was effective in reducing short-term traffic-related air pollution and improving air quality promptly, which could be considered as a feasible alternative in pollution control and air quality assurance in megacities of China like Beijing under particular or emergency occasions.

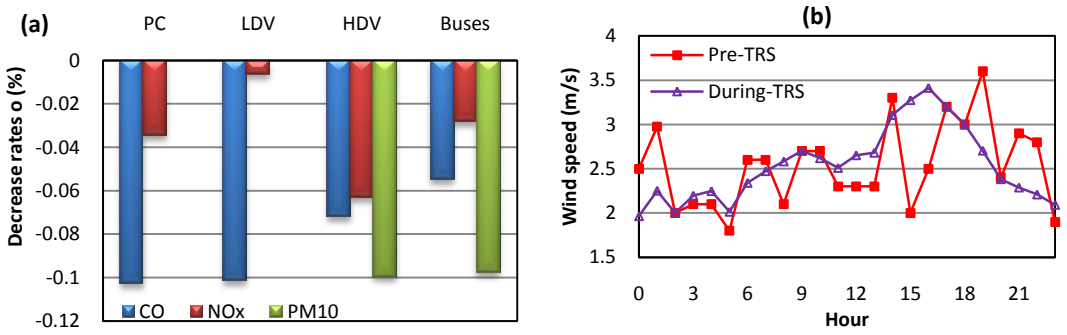

Fig. 11. Air quality impacts during the Games of (a): Reduction rates of emission factors of CO, PM_{10} and NO_x from various vehicle types resulting from the raise of running speed from 20 km/h to 23 km/h, calculated by COPERT model; (b) Variation of wind speed (m/s) on hourly average for the pre-TRS and during-TRS periods.

4. Conclusions

1001 We conducted a modelling evaluation of the air quality impacts of the odd-even day
1002 traffic restriction scheme implemented by the Beijing Municipal Government during
1003 the 2008 Olympic Games, and proved that this policy was effective in reducing
1004 short-term traffic-related air pollution and substantially improved the air quality in the
1005 urban area of Beijing during the Games.

1006 The ADMS-Urban was well evaluated with hourly observations from a
1007 traffic-representative air quality monitoring station, and produced satisfactory
1008 predictions, based on the high temporal resolution on-road traffic flow data retrieved
1009 from the ITS-TAP monitoring network covering the 2^{nd}, 3^{rd}, 4^{th} RR and the LRs
1010 distributing over the major UAB, and on the hourly meteorological data from a
1011 representative Observatory. This study demonstrated that modelling-based air
1012 quality evaluation was a reliable approach and was especially useful for simultaneous
1013 and intensive assessment of air quality responses at multi-receptor and in different
1014 regions of the study domain. However, the possible drawback of using one
1015 traffic-representative station for model evaluation in this study was that the model
1016 predictions in areas away from the simulated roads might have some unknown
1017 uncertainty.

1018 Both daily average and maximum concentrations of CO, PM_{10}, NO_2 and O_3 during
1019 the pre-TRS period deceased significantly to much lower levels during the TRS
1020 period, with the daily average concentrations from on-road vehicles conforming to the
1021 CNAAQS Grade II. However, pollutant concentrations of CO, PM_{10} and NO_2

increased for the post-TRS period, with the exception for O_3 concentration, which continued decreasing, mainly due to the "VOC-limited" characteristic for ozone formation in UAB. The bouncing of pollutant concentration levels of CO, PM_{10} and NO_2 after the expiration of the TRS policy just reversely reflected the effectiveness of the TRS in improving short-term air quality.

The hourly average, especially the peak concentrations of CO, PM_{10}, NO_2 and O_3 were reduced significantly in response to the TRS policy. However, the TRS policy did not change the typical two-peak diurnal variation pattern of the primary pollutants (CO and PM_{10}). Besides, no remarkable weekly variation of pollutant concentrations were revealed as a result of the TRS policy, with the concentration levels of CO, PM_{10}, NO_2 on weekday generally higher than those on weekends. Particularly, a notable ozone weekend effect with higher concentrations on weekends was revealed, mostly due to the decreased NO_x emissions on weekends and the "VOC-limited" characteristic for ozone formation in UAB. Meanwhile, a remarkable reduction of peak hour and daily average concentrations of O_3 was achieved in response to the TRS policy.

Notable air quality improvement was revealed around UAB during the Games, which indicated the overall effectiveness of the TRS policy. Particularly, better effect on pollution reduction was observed in the previously most severely polluted areas, where the concentration level decreased sufficiently to comply with the CNAAQS guidelines. Besides, significant air quality improvement was achieved in

1043 the upwind eastern and southern areas in response to the TRS policy. In conclusion,
1044 the TRS policy was effective in significantly improving short-term and regional air
1045 quality in UAB during the Games, and provided valuable experiences for future
1046 temporary and regional control of traffic-related air pollution.

1047 *Acknowledgements.* This work was supported by the financial support from the
1048 Research on Optimizing the Stationing of Monitoring Sites for Urban Ambient Air
1049 Quality (No. 200709001), from the Research on Photochemical Smog Pollution and
1050 Public Prewarning Standards in Key Cities (No. 200800034), from Shanghai Tongji
1051 Gao Ting-yao Environmental Science and Technology Development Foundation, and
1052 from the Doctoral Thesis Scholarship of China Development Research Foundation
1053 funded by General Motors.

1054 **References**

1055 Assael, M. J., Delaki, M., and Kakosimos, K. E.: Applying the OSPM model to the
1056 calculation of PM_{10} concentration levels in the historical centre of the city of
1057 Thessaloniki, Atmos. Environ., 42, 65-77, 2008.

1058 Atkinson-Palombo, C. M., Miller, J. A., and Balling, R. C.: Quantifying the ozone
1059 "weekend effect" at various locations in Phoenix, Arizona, Atmos. Environ., 40,
1060 7644-7658, 2006.

1061 BeijingAir: http://www.beijingairquality.cn, 2008.

1062 Beijing Municipal Environmental Protection Bureau: Beijing Environmental Bulletin,

1063 http://www.bjepb.gov.cn, 2009.

1064 Bennett, M., and Hunter, G. C.: Some comparisons of lidar estimates of peak
1065 ground-level concentrations with the predictions of UK-ADMS, Atmos. Environ.,
1066 31, 429-439, 1997.

1067 Berkowicz, R.: OSPM - a parameterised street pollution model, Environ. Monit.
1068 Assess., 65, 323-331, 2000.

1069 Berkowicz, R., Ketzel, M., Jensen, S. S., Hvidberg, M., and Raaschou-Nielsen, O.:
1070 Evaluation and application of OSPM for traffic pollution assessment for a large
1071 number of street locations, Environ. Modell. Softw., 23, 296-303, 2008.

1072 Cai, H., and Xie, S. D.: Estimation of vehicular emission inventories in China from
1073 1980 to 2005, Atmos. Environ., 41, 8963-8979, 2007.

1074 Cai, H., and Xie, S. D.: Tempo-spatial variation of emission inventories of speciated
1075 volatile organic compounds from on-road vehicles in China, Atmos. Chem. Phys.,
1076 9, 6983-7002, 2009.

1077 Cambridge Environmental Research Consultants: Validation and sensitivity study of
1078 ADMS-Urban for London,
1079 http://www.cerc.co.uk/environmental-research/assets/data/CERC_2003_ADMS-
1080 Urban_validation_and_sensivity_study_for_London_10_TR-0191-h.pdf, 2003.

1081 Cambridge Environmental Research Consultants: Modelling dry deposition,
1082 http://www.cerc.co.uk/environmental-software/assets/data/doc_techspec/CERC_
1083 ADMS4_P17_13.pdf, 2009.
1084 Cambridge Environmental Research Consultants, http://www.cerc.co.uk, 2009.
1085 Carruthers, D. J., Holroy, D. R. J., Hunt, J. C. R., Weng, W. S., Robins, A. G., Apsley,
1086 D. D., Thomson, D. J., and Smith, F. B.: UK-ADMS - a new approach to
1087 modeling dispersion in the earth's atmospheric boundary-layer, J. Wind. Eng. Ind.
1088 Aerod., 52, 139-153, 1994.
1089 Carruthers, D. J., Mckeown, A. M., Hall, D. J., and Porter, S.: Validation of ADMS
1090 against wind tunnel data of dispersion from chemical warehouse fires, Atmos.
1091 Environ., 33, 1937-1953, 1999.
1092 Carruthers, D. J., Dyster, S., and McHugh, C. A.: Contrasting methods for validating
1093 ADMS using the Indianapolis dataset, Int. J. Environ. Pollut., 14, 115-121,
1094 2000a.
1095 Carruthers, D. J., Edmunds, H. A., Lester, A. E., McHugh, C. A., and Singles, R. J.:
1096 Use and validation of ADMS-Urban in contrasting urban and industrial locations,
1097 Int. J. Environ. Pollut., 14, 364-374, 2000b.
1098 Carruthers, D. J., Dickson, P., McHugh, C. A., Nixon, S. G., and Oates, W.:
1099 Determination of compliance with UK and EU air quality objectives from
1100 high-resolution pollutant concentration maps calculated using ADMS-Urban, Int.

1101 J. Environ. Pollut., 16, 460-471, 2001.

1102 CERC. ADMS-Urban User Guide. CERC Limited, Cambridge, February 1999.

1103 Chan, C. K., and Yao, X.: Air pollution in mega cities in China, Atmos. Environ., 42,
1104 1-42, 2008.

1105 Cheng, Y. F., Heintzenberg, J., Wehner, B., Wu, Z. J., Su, H., Hu, M., and Mao, J. T.:
1106 Traffic restrictions in Beijing during the Sino-African Summit 2006: aerosol size
1107 distribution and visibility compared to long-term in situ observations, Atmos.
1108 Chem. Phys., 8, 7583–7594, 2008.

1109 Chinese Olympic Committee: The temporary traffic control implementations for
1110 non-Beijing local vehicles during 2008 Beijing Olympic and Paralympic Games,
1111 http://www.beijing2008.cn/news/olympiccities/beijing/n214412173.shtml, 20
1112 June, 2008.

1113 Chou, C. C. K., Liu, S. C., Lin, C. Y., Shiu, C. J., and Chang, K. H.: The trend of
1114 surface ozone in Taipei, Taiwan, and its causes: Implications for ozone control
1115 strategies, Atmos. Environ., 40, 3898-3908, 2006.

1116 McHugh, C., Carruthers, D., Sheng, X.Y.: Using ADMS models for air quality
1117 assessment and management in China, Cambridge Environmental Research
1118 Consultants (CERC), Chinese. J. Popul. Resour. Environ., 3, 2005.

1119 Derwent, R.G., and Middleton, D.R.: An empirical function for the ratio NO_2/NO_x.
1120 Clean Air (NSCA) 26, 57–60, 1996.

1121 Elbir, T.: Application of an ISCST3 model for predicting urban air pollution in the
1122 Izmir metropolitan area, Int. J. Environ. Pollut., 18, 498-507, 2002.

1123 European Environment Agency: COPERT III-Computer programme to calculate
1124 emissions from road transport, methodology and emission factors (version 2.1),
1125 technical report No. 49, 2000.

1126 Fang, M., Chan, C. K., and Yao, X. H.: Managing air quality in a rapidly developing
1127 nation: China, Atmos. Environ., 43, 79-86, 2009.

1128 Gao, H. O., and Niemeier, D. A.: The impact of rush hour traffic and mix on the ozone
1129 weekend effect in southern California, Transport. Res. D-Tr. E., 12, 83-98, 2007.

1130 Granell, J., Ho, C., Tang, T., and Roberts, M.: Analysis of MOBILE6.2's PM emission
1131 factor estimating function, USEPA's 13th International Emission Inventory
1132 Conference "Working for Clean Air in Clearwater",
1133 http://www.epa.gov/ttn/chief/conference/ei13/mobile/granell.pdf, 2004.

1134 Hanna, S.R., Strimaitis, D.G., and Chang, J.C.: Hazard response modeling uncertainty
1135 (A quantitative method), 1991.

1136 Hanna, S.R., Chang, J.C., and Strimaitis, D.G.: Hazardous gas model evaluation with
1137 field observations, Atmos. Environ., 27, 2265–2285, 1993.

1138 Hao, J. M., Wu, Y., Fu, L. X., He, D. Q., and He, K. B.: Source contributions to
1139 ambient concentrations of CO and NOx in the urban area of Beijing, J. Environ.
1140 Sci. Heal. A - Toxic/Hazard. Subst. Environ. Eng., 36, 215-228, 2001.

1141 Hirtl, M., and Baumann-Stanzer, K.: Evaluation of two dispersion models
1142 (ADMS-Roads and LASAT) applied to street canyons in Stockholm, London and
1143 Berlin, Atmos. Environ., 41, 5959-5971, 2007.

1144 Hu, F.: Turbulence interval and atmospheric boundary layer [D], Ph.D dissertation (in
1145 Chinese), Institute of Atmospheric Physics, Chinese Academy of Sciences, 1994.

1146 Kenty, K. L., Poor, N. D., Kronmiller, K. G., McClenny, W., King, C., Atkeson, T.,
1147 and Campbell, S. W.: Application of CALINE4 to roadside NO/NO_2
1148 transformations, Atmos. Environ., 41, 4270-4280, 2007.

1149 Khoder, M. I.: Diurnal, seasonal and weekdays-weekends variations of ground level
1150 ozone concentrations in an urban area in greater Cairo, Environ. Monit. Assess.,
1151 149, 349-362, 2009.

1152 Kukkonen, J., Valkonen, E., Walden, J., Koskentalo, T., Aarnio, P., Karppinen, A.,
1153 Berkowicz, R., and Kartastenpaa, R.: A measurement campaign in a street
1154 canyon in Helsinki and comparison of results with predictions of the OSPM
1155 model, Atmos. Environ., 35, 231-243, 2001.

1156 Levitin, J., Harkonen, J., Kukkonen, J., and Nikmo, J.: Evaluation of the CALINE4
1157 and car-fmi models against measurements near a major road, Atmos. Environ.,
1158 39, 4439-4452, 2005.

1159 Liu, J., Zhang, X.L., Xie, P., Dong, F., Ouyang, J., and Wang, Z.F.: The variation
1160 characteristics of trace reactive gases at Shangdianzi regional background

monitoring station, Environ. Chem. (in Chinese), 26 (5): 693-698, 2007.

Liu, J., Zhang, X.L., Xu, X.F., and Xu, H.H.: Comparison analysis of variation characteristics of SO_2, NO_x, O_3 and $PM_{2.5}$ between rural and urban areas, Beijing, Environ. Science. (in Chinese), 29 (4): 1059-1065, 2008.

Liu, J., Zhang, X.L., Zhang, X.C., and Tang, J.: Surface ozone characteristics and the correlated factors at Shangdianzi atmospheric background monitoring station, Res. Environ. Sciences. (in Chinese), 19 (4): 19-25, 2006.

Liu, X.M., Hu, and F., Li, L.: Analyses on the characteristics of Beijing summer urban heat island and its meteorological fields (in Chinese), J. Grad. School. Chinese. Acad. Sci., 23, 70-76, 2006.

Lu, L.H., Bian, L.G., Cheng, Y.J., Gao, Z.Q., and Wang, Y.: Meteorological Characteristics of the ground layer in Beijing in winter, J. Appl. Meteorol. Science. (in Chinese), 13 (Suppl.): 34-42, 2002.

McHugh, C. A., Carruthers, D. J., and Edmunds, H. A.: ADMS-Urban: An air quality management system for traffic, domestic and industrial pollution, Int. J. Environ. Pollut., 8, 666-674, 1997.

Miao, S.G., Chen, F., Margaret, A.L., Mukul, T., Li, Q.C., and Wang, Y.C.: An observational and modeling study of characteristics of urban heat island and boundary layer structures in Beijing, J. Appl. Meteorol. Clim., 48, 484-501, 2008.

1181 Ministry of Environmental Protection of the People's Republic of China: Disposition
1182 of banning of biomass burning for the air quality assurance during the Games,
1183 http://test.mep.gov.cn/ztbd/sjhjr/0865/lsay/200805/t20080529_123206.htm (in
1184 Chinese), 2008.

1185 Ministry of Environmental Protection of the People's Republic of China, Guidelines
1186 for environmental impact assessment - atmospheric environment, pp 24, 2009.

1187 Murphy, J. G., Day, D. A., Cleary, P. A., Wooldridge, P. J., Millet, D. B., Goldstein, A.
1188 H., and Cohen, R. C.: The weekend effect within and downwind of Sacramento -
1189 Part 1: Observations of ozone, nitrogen oxides, and VOC reactivity, Atmos.
1190 Chem. Phys., 7, 5327-5339, 2007.

1191 NARSTO: An assessment of tropospheric ozone pollution: A North American
1192 perspective, The NARSTO Synthesis Team, Palo Alto, CA, 2000.

1193 NASA, http://aura.gsfc.nasa.gov/science/china.html, 2009.

1194 Okuda, T., Kato, J., Mori, J., Tenmoku, M., Suda, Y., Tanaka, S., He, K., Ma, Y.,
1195 Yang, F., Yu, X., and Duan, F.: Daily concentrations of trace metals in aerosols
1196 in Beijing, China, determined by using inductively coupled plasma mass
1197 spectrometry equipped with laser ablation analysis, and source identification of
1198 aerosols, Sci. Total Environ., 330 (1-3), 145-158, 2004.

1199 Olesen, H.R.: Ten years of harmonization activities: past, present, and future. 7th Int.
1200 Conf. on Harmonisation within Atmospheric Dispersion Modelling for

1201 Regulatory Purposes, Belgirate, Italy, National Environmental Research Institute,
1202 Roskilde, Denmark, www.harmo.org, 2001.

1203 Riddle, A., Carruthers, D., Sharpe, A., McHugh, C., and Stocker, J.: Comparisons
1204 between fluent and ADMS for atmospheric dispersion modelling, Atmos.
1205 Environ., 38, 1029-1038, 2004.

1206 Sadanaga, Y., Shibata, S., Hamana, M., Takenaka, N., and Bandow, H.:
1207 Weekday/weekend difference of ozone and its precursors in urban areas of Japan,
1208 focusing on nitrogen oxides and hydrocarbons, Atmos. Environ., 42, 4708-4723,
1209 2008.

1210 Sharma, S., and Chandra, A.: Simulation of air quality using an ISCST3 dispersion
1211 model, Clean-Soil. Air. Water., 36, 118-124, 2008.

1212 Song, Y., Tang, X.Y., Xie, S.D., Zhang, Y.H., Wei, Y.J., Zhang, M.S., Zeng, L.M.,
1213 and Lu, S.H.: Source apportionment of PM2.5 in Beijing in 2004, J. Hazard.
1214 Mater., 146, 124-130, 2007.

1215 Song, Y., Zhang, M.S., Cai, X.H.: PM10 modeling of Beijing in winter, Atmos.
1216 Environ., 40 (22), 4126-4136, 2006a.

1217 Song, Y., Zhang, Y.H., Xie, S.D., Zeng, L.M., Zheng, M., Salmon, L.G., Shao, M.,
1218 and Slanina, S.: Source apportionment of PM2.5 in Beijing by positive matrix
1219 factorization, Atmos. Environ., 40 (8), 1526-1537, 2006b.

1220 Sun, Y.L., Zhuang, G.S., Wang, Y., Han, L.H., Guo, J.H., Dan, M., Zhang, W.J.,

1221 Wang, Z.F. and Hao, Z.P.: The air-borne particulate pollution in
1222 Beijing-concentration, composition, distribution and sources, Atmos. Environ.,
1223 38 (35), 5991-6004, 2004.

1224 Streets, D.G., Fu, J.S., Jang, C.J., Hao, J.M., He, K.B., Tang, X.Y., Zhang, Y.H.,
1225 Wang, Z.F., Li, Z.P., Zhang, Q., Wang, L.T., Wang, B.Y., and Yu, C.: Air
1226 quality during the 2008 Beijing Olympic Games, Atmos. Environ., 41 (3),
1227 480-492, 2007.

1228 Tang, W. Y., Zhao, C. S., Geng, F. H., Peng, L., Zhou, G. Q., Gao, W., Xu, J. M., and
1229 Tie, X. X.: Study of ozone "weekend effect" in Shanghai, Sci China Ser D, 51,
1230 1354-1360, 2008.

1231 Vardoulakis, S., Valiantis, M., Milner, J., and ApSimon, H.: Operational air pollution
1232 modelling in the UK-Street canyon applications and challenges, Atmos. Environ.,
1233 41, 4622-4637, 2007.

1234 Venkatram, A., Karamchandani, P.O., Pai, P., Goldstein, R.: The development and
1235 application of a simplified ozone modelling system, Atmos. Environ., 28,
1236 3665-3678, 1994.

1237 Wang, B.G., Zhang, Y.H., Wu, Z.Q., Chan, L.Y.: Tunnel test for motor vehicle
1238 emission factors in Guangzhou, Res. Environ. Sci., 14, 13-16, 2001.

1239 Wang, H.L., Zhuang, Y.H., Wang, Y., Sun, Y.L., Yuan, H., Zhuang, G.S., and Hao,
1240 Z.P.: Long-term monitoring and source apportionment of $PM_{2.5}$/PM_{10} in Beijing,

1241 China, J. Environ. Sci. - China, 20, 1323-1327, 2008b.

1242 Wang, L. J., Parker, D. B., Parnell, C. B., Lacey, R. E., and Shaw, B. W.: Comparison
1243 of Calpuff and ISCST3 models for predicting downwind odor and source
1244 emission rates, Atmos. Environ., 40, 4663-4669, 2006.

1245 Wang, L.T., Hao, J.M., He, K.B., Wang, S.X., Li, J.H., Zhang, Q., Streets, D.G., Fu,
1246 J.S., Jang, C.J., Takekawa, H., and Chatani, S.: A modeling study of coarse
1247 particulate matter pollution in Beijing: Regional source contributions and control
1248 implications for the 2008 Summer Olympics, J. Air. Waste. Manag. Assoc., 58
1249 (8), 1057-1069, 2008a.

1250 Wang, T. and Xie, S.D.: Assessment of traffic-related air pollution in the urban streets
1251 before and during the 2008 Beijing Olympic Games traffic control period, Atmos.
1252 Environ., 43 (35), 5682-5690, 2009.

1253 Wang, W.X., Chai, F.H., Zhang, Kai., Wang, S.L., Chen, Y.Z., Wang, X.Z., and Yang,
1254 Y.Q.: Study on ambient air quality in Beijing for the summer 2008 Olympic
1255 Games, Air. Qual. Atmos. Health., 1 (1), 31-36, 2008c.

1256 Wang, X., Westerdahl, D., Chen, L. C., Wu, Y., Hao, J. M., Pan, X. C., Guo, X. B.,
1257 and Zhang, K. M.: Evaluating the air quality impacts of the 2008 Beijing
1258 Olympic Games: On-road emission factors and black carbon profiles, Atmos.
1259 Environ., 43 (30), 4535-4543, 2009a.

1260 Wang, X. S., and Li, J. L.: The contribution of anthropogenic hydrocarbons to ozone

1261 formation in Beijing areas (in Chinese), China Environ Sci, 22, 501-505, 2002.

1262 Wang, X. S., Li, J. L., Zhang, Y. H., Xie, S. D., and Tang, X. Y.: Ozone source
1263 attribution during a severe photochemical smog episode in Beijing, China, Sci.
1264 China. Ser. B-Chem., 52, 1270-1280, 2009c.

1265 Wang, Y., Hao, J., McElroy, M. B., Munger, J. W., Ma, H., Chen, D., and Nielsen, C.
1266 P.: Ozone air quality during the 2008 Beijing Olympics: Effectiveness of
1267 emission restrictions, Atmos. Chem. Phys., 9, 5237-5251, 2009b.

1268 WHO: World Health Organization Air Quality Guidelines Global Update,
1269 http://www.euro.who.int/air/activities/20050222_2, 2005.

1270 Willmott, C.J.: Some comments on the evaluation of model performance, Bull. Amer.
1271 Meteor. Soc. 63, 1309–1313, 1982.

1272 Wu, Y., Hao, J.M., Fu, L.X., Wang, Z.S., Tang, U.: Vertical and horizontal profiles of
1273 airborne particulate matter near major roads in Macao, China. Atmos. Environ.,
1274 36 (31), 4907-4918, 2002.

1275 Xie, S. D., Liu, Z., Chen, T., and Hua, L.: Spatiotemporal variations of ambient PM_{10}
1276 source contributions in Beijing in 2004 using positive matrix factorization,
1277 Atmos. Chem. Phys., 8, 2701-2716, 2008.

1278 Ying, G. X., Ma, J., and Xing, Y.: Comparison of air quality management strategies of
1279 PM_{10}, SO_2, and NO_x, by an industrial source complex model in Beijing, Environ.
1280 Prog., 26, 33-42, 2007.

1281 Yura, E. A., Kear, T., and Niemeier, D.: Using CALINE dispersion to assess vehicular
1282 $PM_{2.5}$ emissions, Atmos. Environ., 41, 8747-8757, 2007.

1283 Zhang, H.S. and Chen, J.Y.: Estimation of aerodynamic parameters on nonsingle
1284 horizontal homogeneous underlying surface, Journal of Applied Meteorological
1285 Science (in Chinese), 8 (3): 310-315, 1997.

1286 Zhang, W., Guo, J.H., Sun, Y.L., Yuan, H., Zhuang, G.S., Zhuang, Y.H., and Hao,
1287 Z.P.: Source apportionment for urban PM_{10} and $PM_{2.5}$ in the Beijing area,
1288 Chinese Science Bulletin, 52 (5), 608-615, 2007.

1289 Zheng, M., Salmon, L.G., Schauer, J.J., Zeng, L.M., Kiang, C.S., Zhang, Y.H., and
1290 Cass, G.R.: Seasonal trends in PM2.5 source contributions in Beijing, China,
1291 Atmos. Environ., 39 (22), 3967-3976, 2005.